# CHAPTER 3

# Results and Discussion

## 3.1 Preliminary Studies of Spectrophotometric Determination of Iron (III) Using Eriochrome Cyanine R as a Complexing Agent

### 3.1.1 Absorption spectra

The absorption spectra of ECR, ECR-CTMAB, Fe-ECR and Fe-ECR-CTMAB complexes against water were scanned over a range from 400-700 nm, using JENWAY 6400 spectrophotometer (Figure 3.1). The ternary complex exhibited an absorption maximum at 610 nm. Therefore, all measurements were made at this wavelength.

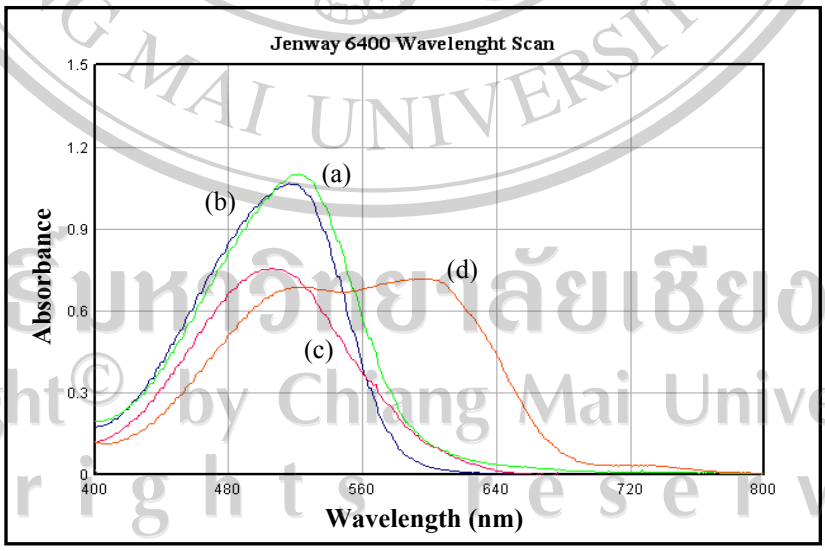


**Figure 3.1** Absorption spectra of: (a) ECR, (b) ECR-CTMAB, (c) Fe (III)-ECR and (d) Fe (III)-ECR-CTMAB complex against water at pH 4.0.

### 3.1.2 Mole-ratio method

To study the composition of Fe-ECR-CTMAB ternary complex, used the mole ratio method. In this method, a series of solution are prepared containing a fixed amount of metal ion, with a varying concentration of ligand. The absorbances of these solutions are then measured. A resulting plot of absorbance vs. ligand-to-metal ratio initially increases, and then becomes constant one the ligand to metal ratio has been achieved. The point at which the slope of the line changes corresponds to the ligand: metal ratio of the complex [68]. The mole-ratio methods of Fe-ECR-CTMAB complex was defined as 2 series of solution were prepared in which iron and CTMAB concentrations were fix while the ECR concentration was varied. Another one is prepared in which iron and ECR concentrations were fixed while the CTMAB concentration was varied.

Series I; the various concentrations of ECR were added to solution containing $1\times10^{-5}$ mol $L^{-1}$ of iron, $1\times10^{-4}$ mol $L^{-1}$ CTMAB, 5 mL of 0.5 mol $L^{-1}$ of acetate buffer pH 4.0 and diluted with deionized water in 25 mL volumetric flasks. Absorbance of each solution was measured at 610 nm. The results were shown in Table 3.1 and Figure 3.2. It was found that the absorbance as peak height increased to maximum at concentration of ECR was $2\times10^{-5}$ mol $L^{-1}$ and then it became constant and so did the absorbance as AU. Therefore, $2\times10^{-5}$ mol $L^{-1}$ of ECR concentration was chosen for studied effect of CTMAB concentration in series II.

**Table 3.1** Effect of ECR concentrations for mole-ratio Fe-ECR-CTMAB complex.

| [ECR] ( x $10^{-5}$ mol $L^{-1}$) | Mole ratio (Fe:ECR) | Absorbance (AU)* |
|---|---|---|
| 0 | 1:0 | 0.020 |
| 1 | 1:1 | 0.280 |
| 2 | 1:2 | 0.400 |
| 3 | 1:3 | 0.419 |
| 4 | 1:4 | 0.423 |
| 5 | 1:5 | 0.425 |
| 6 | 1:6 | 0.427 |

*average of triplicate results

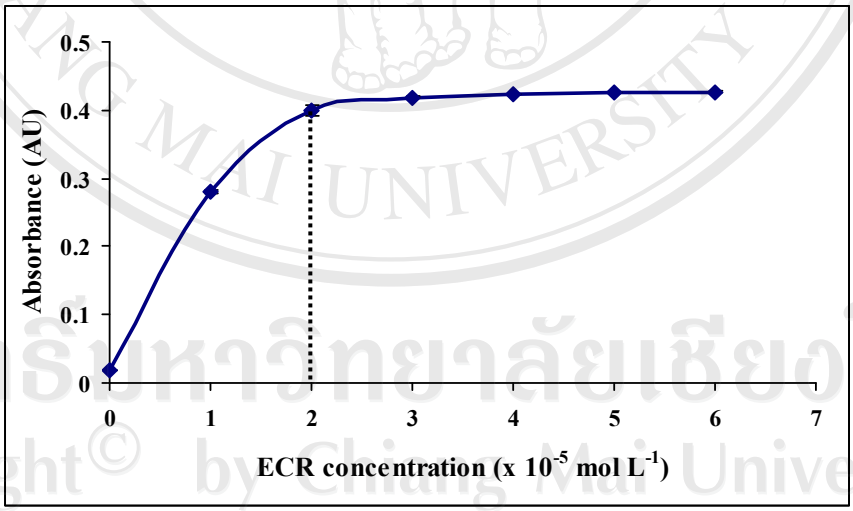


**Figure 3.2** Mole-ratio study of Fe-ECR-CTMAB system; effect of ECR concentration. Fe $1\times10^{-5}$ mol $L^{-1}$, CTMAB $1\times10^{-5}$ mol $L^{-1}$, pH 4.0, wavelength 610 nm.

Series II ; the various concentrations of CTMAB were added to solution containing $1\times10^{-5}$ mol $L^{-1}$ of iron, $2\times10^{-5}$ mol $L^{-1}$ of ECR, 5 mL of 0.5 mol $L^{-1}$ of acetate buffer pH 4.0 and diluted with deionized water in 25 mL volumetric flasks. Absorbance of each solution was measured at 610 nm. The results are shown in Table 3.2 and Figure 3.3. It was found that the absorbance as peak height increased to maximum up to the CTMAB concentration of $4\times10^{-5}$ mol $L^{-1}$ then it became constant and so did the absorbance in AU. Therefore, $4\times10^{-5}$ mol $L^{-1}$ CTMAB concentration was chosen.

**Table 3.2** Effect of CTMAB concentrations for mole-ratio Fe-ECR-CTMAB complex.

| **[CTMAB] ( x $10^{-5}$ mol $L^{-1}$)** | **Mole ratio (Fe:ECR:CTMAB)** | **Absorbance (AU)*** |
|---|---|---|
| 0 | 1:2:0 | 0.098 |
| 1 | 1:2:1 | 0.238 |
| 2 | 1:2:2 | 0.396 |
| 3 | 1:2:3 | 0.521 |
| 4 | 1:2:4 | 0.647 |
| 5 | 1:2:5 | 0.657 |
| 6 | 1:2:6 | 0.659 |
| 7 | 1:2:7 | 0.662 |
| 8 | 1:2:8 | 0.665 |
| 9 | 1:2:9 | 0.668 |

*average of triplicate results

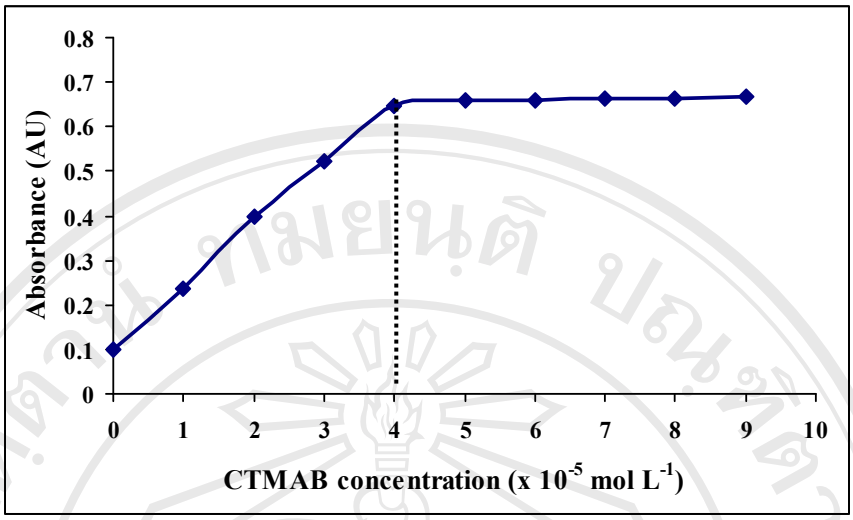


**Figure 3.3** Mole-ratio study of Fe-ECR-CTMAB system; effect of CTMAB concentration. Fe $1\times10^{-5}$ mol $L^{-1}$, ECR $2\times10^{-5}$ mol $L^{-1}$, pH 4.0, wavelength 610 nm.

From experimental results in Tables 3.1 and 3.2 and Figures 3.2 and 3.3 gave a mole-ratio of Fe: ECR: CTMAB at 1:2:4. So, the reaction of Fe-ECR-CTMAB complex may be exactly the same as reaction of Fe-ECR-CTMAB [61]. The reaction of Fe-ECR-CTMAB was shown in Figure 3.4.

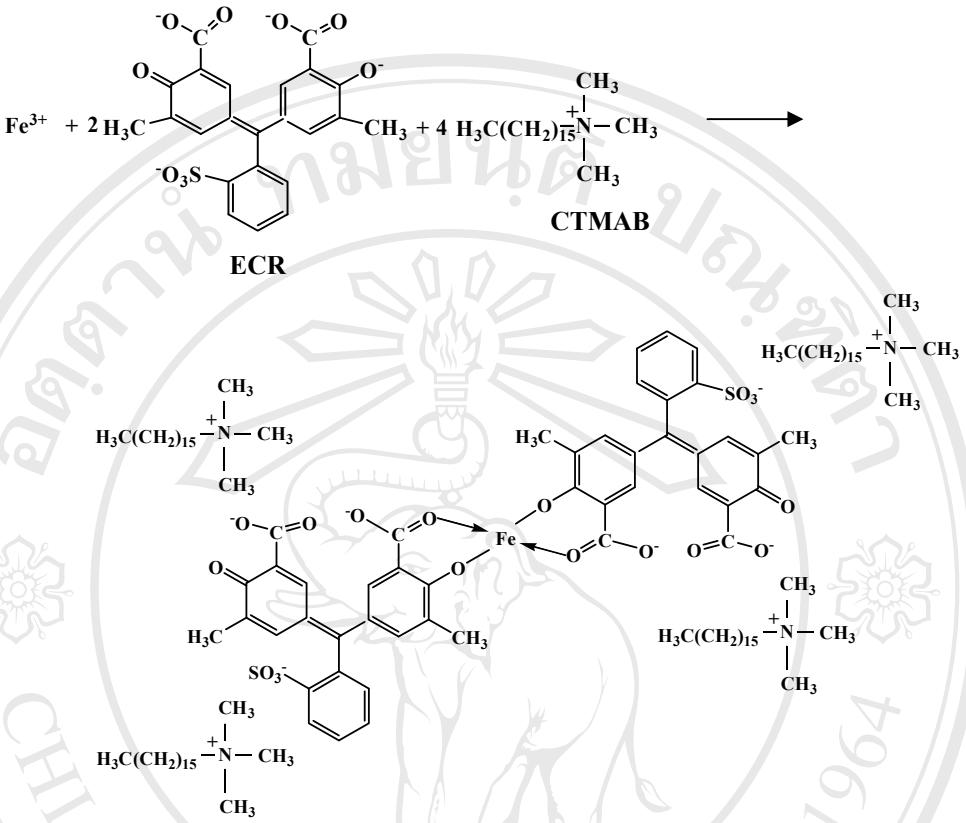


**Figure 3.4** The reaction of Fe-ECR-CTMAB [61].

## 3.2 FIA spectrophotometric Determination of Iron (III) Using Eriochrome Cyanine R and Cetyltrimethyl Ammonium Bromide as A Complexing Agent

### 3.2.1 Optimization of the Flow System by Univariate Method

The conditions for the determination of iron (III) were optimized by studying the influences of the various parameters, such as wavelength, pH concentration of ECR and CTMAB, flow rate, reaction coil, and sample loop, respectively. The optimum conditions obtained by means of the univariate optimization procedure (changing one variable in turn and keeping the others at their optimum values). All optimum values were chosen by judging from the greatest peak height, stability of the base line, low or no positive blank signals, low analysis time, availability and economy. To optimize the conditions, the FIA manifold in Figure 2.1 and the preliminary experimental conditions (Table 2.2) were used.

#### 3.2.1.1 Optimum wavelength

The optimum wavelength for iron determination was studied over the range 595-625 nm by the proposed FIA system (Fig 2.3) using the experimental conditions as shown in Table 2.2. The results shown in Table 3.3 and Figure 3.5 indicated that the highest sensitivity of the method (defined as slope of calibration curve) was obtained when the absorbance was measured at 610 nm. The analytical wavelength at 610 nm was selected for the further studies.

**Table 3.3** Effect of wavelength on the sensitivity.

| Wavelength (nm) | ΔP.H.* (AU) obtained from the standard Fe(III) (mg $L^{-1}$) | | | y = mx + c | $r^2$ |
|---|---|---|---|---|---|
| | 0.1 | 0.2 | 0.3 | | |
| 595 | 0.013 | 0.040 | 0.063 | y = 0.2517x - 0.0118 | 0.9975 |
| 600 | 0.014 | 0.042 | 0.065 | y = 0.2533x - 0.0104 | 0.9963 |
| 605 | 0.015 | 0.043 | 0.066 | y = 0.2550x - 0.0098 | 0.9976 |
| 610 | 0.017 | 0.044 | 0.071 | y = 0.2750x - 0.0103 | 0.9999 |
| 615 | 0.019 | 0.046 | 0.070 | y = 0.2567x - 0.0062 | 0.9991 |
| 620 | 0.021 | 0.046 | 0.070 | y = 0.2450x - 0.0036 | 0.9996 |
| 625 | 0.014 | 0.036 | 0.056 | y = 0.2100x - 0.0063 | 0.9992 |

*average of triplicate results

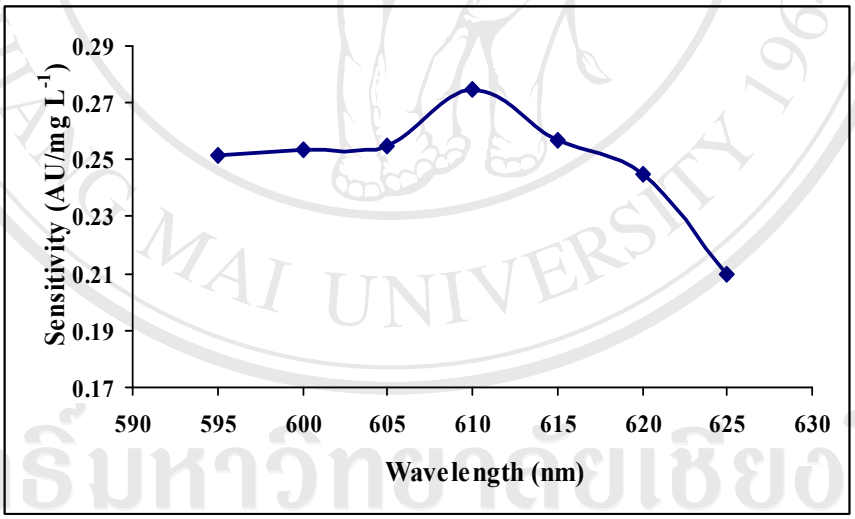


**Figure 3.5** Relationship between wavelength and sensitivity of the calibration curve.

### 3.2.1.2 Effect of pH on sensitivity

The complexation of Fe-ECR-CTMAB was studied at different pH values in the range of 3.5-7.5. The pH values of buffer solution were adjusted with acetic acid/sodium acetate. Using the manifold as shown in figure 2.1, a 0.1 mol $L^{-1}$ of acetate buffer solution was mixed in solution of ECR and CTMAB. The results, which are presented in Table 3.4 and Figure 3.6 display that Fe $(ECR)_2$ in CTMAB media complex showed the maximum sensitivity at pH 4.5. In higher pH, mixed complexes Fe-ECR and $OH^-$ could be formed or due to probable hydroxide precipitation sensitivity will be decreased. On the other hand, at lower pH because of ligand protonation decrease in sensitivity will be observed. In subsequent work, pH 4.5 has been selected.

**Table 3.4** Effect of pH on the sensitivity.

| pH | ΔP.H.* (AU) obtained from the standard Fe(III) (mg $L^{-1}$) | | | | | y = mx + c | $r^2$ |
|---|---|---|---|---|---|---|---|
| | 0.1 | 0.15 | 0.2 | 0.25 | 0.3 | | |
| 3.5 | 0.012 | 0.016 | 0.020 | 0.024 | 0.027 | y = 0.0038x + 0.0082 | 0.9953 |
| 4.0 | 0.033 | 0.053 | 0.069 | 0.082 | 0.096 | y = 0.3093x + 0.0047 | 0.9924 |
| 4.5 | 0.041 | 0.061 | 0.073 | 0.093 | 0.105 | y = 0.3207x + 0.0105 | 0.9935 |
| 5.0 | 0.035 | 0.048 | 0.060 | 0.071 | 0.079 | y = 0.2213x + 0.0144 | 0.9900 |
| 5.5 | 0.024 | 0.033 | 0.041 | 0.050 | 0.059 | y = 0.1733x + 0.0068 | 0.9992 |
| 6.0 | 0.020 | 0.025 | 0.032 | 0.038 | 0.045 | y = 0.1253x + 0.0070 | 0.9982 |
| 6.5 | 0.017 | 0.024 | 0.029 | 0.034 | 0.039 | y = 0.1100x + 0.0067 | 0.9958 |
| 7.0 | 0.015 | 0.021 | 0.026 | 0.031 | 0.035 | y = 0.0987x + 0.0058 | 0.9933 |
| 7.5 | 0.009 | 0.012 | 0.016 | 0.020 | 0.024 | y = 0.0773x + 0.0008 | 0.9962 |

*average of triplicate results

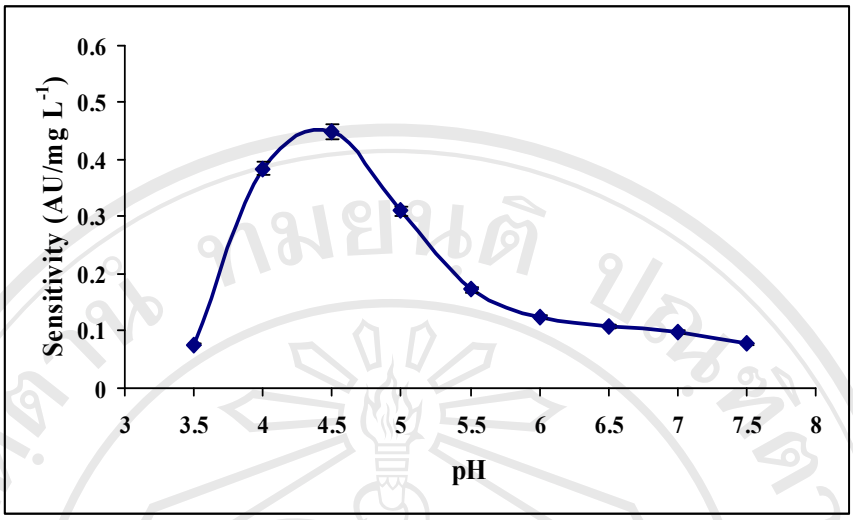


**Figure 3.6** Relationship between pH and sensitivity of the calibration curve.

### 3.2.1.3 Effect of ECR concentration on sensitivity

The Effect of ECR concentrations on the determination of Fe (III) (0.1-0.3 mg $L^{-1}$) was studied in the range $1.0\times10^{-4}$- $5.0\times10^{-4}$ mol $L^{-1}$. The results are shown in Table 3.5 and Figure 3.7. As it can be seen, in the case of the addition of the increased concentrations of ECR to iron (III) solution, the sensitivity of Fe-ECR-CTMAB complex increased and became constant when the ECR concentration increased up to $3.0\times10^{-4}$ mol $L^{-1}$ at 610 nm. For this reason, the present study was carried out with the $3.0\times10^{-4}$ mol $L^{-1}$ of ECR concentration. Results displays that ligand concentration must be exceed that of $Fe^{3+}$ ion concentration to reach effective complexation to achieve high sensitivity.

**Table 3.5** Effect of concentration of ECR on the sensitivity.

| ECR concentration ($\times 10^{-4}$ M) | ΔP.H.* (AU) obtained from the standard Fe(III) (mg $L^{-1}$) | | | | | y = mx + c | $r^2$ |
|---|---|---|---|---|---|---|---|
| | 0.1 | 0.15 | 0.2 | 0.25 | 0.3 | | |
| 1.0 | 0.033 | 0.047 | 0.059 | 0.077 | 0.091 | y = 0.2920x + 0.0030 | 0.9964 |
| 1.5 | 0.030 | 0.044 | 0.064 | 0.079 | 0.089 | y = 0.3073x - 0.0002 | 0.9899 |
| 2.0 | 0.031 | 0.046 | 0.066 | 0.078 | 0.096 | y = 0.3240x - 0.0015 | 0.9965 |
| 2.5 | 0.037 | 0.051 | 0.072 | 0.085 | 0.105 | y = 0.3400x + 0.0020 | 0.9952 |
| 3.0 | 0.028 | 0.046 | 0.068 | 0.081 | 0.100 | y = 0.3580x - 0.0070 | 0.9953 |
| 3.5 | 0.044 | 0.062 | 0.079 | 0.092 | 0.102 | y = 0.2907x + 0.0176 | 0.9854 |
| 4.0 | 0.033 | 0.047 | 0.061 | 0.073 | 0.090 | y = 0.2800x + 0.0048 | 0.9976 |
| 4.5 | 0.020 | 0.036 | 0.049 | 0.059 | 0.072 | y = 0.2540x - 0.0036 | 0.9939 |
| 5.0 | 0.014 | 0.025 | 0.039 | 0.051 | 0.064 | y = 0.2520x - 0.0118 | 0.9990 |

*average of triplicate results

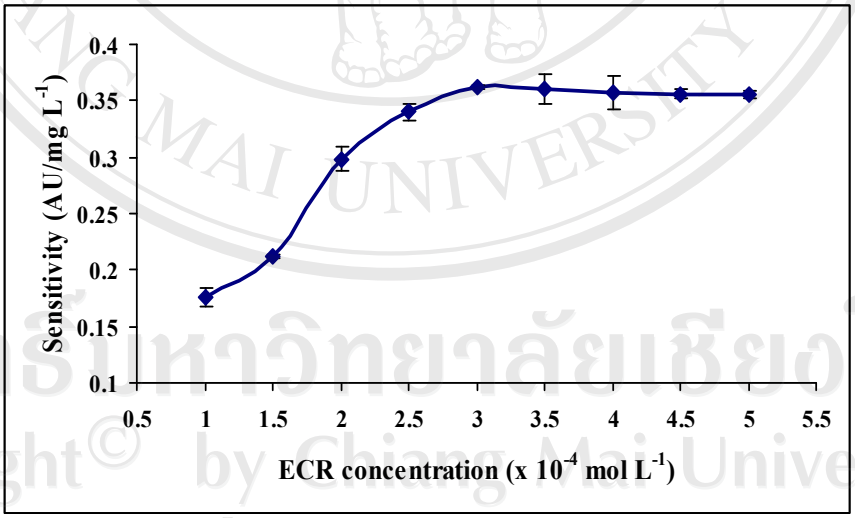


**Figure 3.7** Relationship between concentration of ECR and sensitivity of the calibration curve.

### 3.2.1.4 Effect of CTMAB concentration on sensitivity

The Effect of CTMAB concentration on the determination of Fe (III) (0.1-0.3 mg $L^{-1}$) was studied at different concentration values in the range of $1.0\times10^{-5}$- $3.5\times10^{-3}$ mol $L^{-1}$. The results are shown in Table 3.6 and Figure 3.8. It was found that sensitivity increased very rapidly from the CTMAB concentration of $1.0\times10^{-5}$ - $1.0\times10^{-3}$ mol $L^{-1}$. After that, the sensitivities were decreased. This is due to the fact that increasing the CTMAB concentration leading to the increase in amounts of Fe-ECR-CTMAB complexation which results in a higher sensitivity. However, beyond the CTMAB concentrations of $1.0\times10^{-3}$ mol $L^{-1}$, the absorbance of Fe-ECR-CTMAB complex decreases. Consequently, a concentration of $1.0\times10^{-3}$ mol $L^{-1}$ of CTMAB was chosen as optimum.

**Table 3.6** Effect of concentration of CTMAB on the sensitivity.

| **CTMAB concentration ($\times10^{-3}$ M)** | **ΔP.H.* (AU) obtained from the standard Fe(III) (mg $L^{-1}$)** | | | | | **y = mx + c** | **$r^2$** |
|---|---|---|---|---|---|---|---|
| | **0.1** | **0.15** | **0.2** | **0.25** | **0.3** | | |
| 0.10 | 0.025 | 0.035 | 0.047 | 0.058 | 0.068 | y = 0.2180x + 0.0031 | 0.9988 |
| 0.25 | 0.010 | 0.025 | 0.040 | 0.058 | 0.071 | y = 0.3033x - 0.0201 | 0.9966 |
| 0.50 | 0.039 | 0.056 | 0.073 | 0.092 | 0.111 | y = 0.3613x + 0.0020 | 0.9990 |
| 1.00 | 0.038 | 0.058 | 0.076 | 0.095 | 0.113 | y = 0.3753x + 0.0010 | 0.9998 |
| 1.50 | 0.033 | 0.050 | 0.071 | 0.087 | 0.101 | y = 0.3460x - 0.0008 | 0.9952 |
| 2.00 | 0.031 | 0.046 | 0.063 | 0.079 | 0.095 | y = 0.3220x - 0.0016 | 0.9997 |
| 2.50 | 0.029 | 0.045 | 0.061 | 0.076 | 0.090 | y = 0.3060x - 0.0010 | 0.9992 |
| 3.00 | 0.032 | 0.044 | 0.058 | 0.070 | 0.086 | y = 0.2680x + 0.0044 | 0.9976 |
| 3.50 | 0.028 | 0.042 | 0.055 | 0.069 | 0.081 | y = 0.2653x + 0.0020 | 0.9992 |

*average of triplicate results

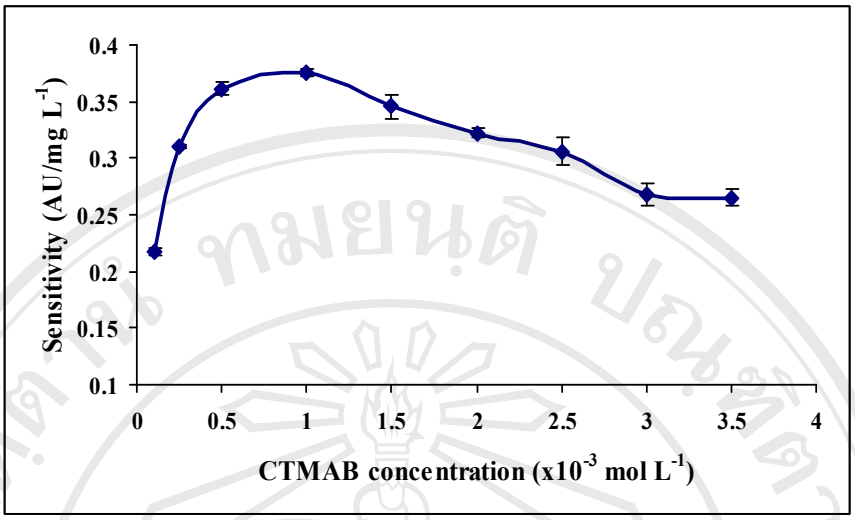


**Figure 3.8** Relationship between concentration of CTMAB and sensitivity of the calibration curve.

### 3.2.1.5 Effect of flow rate on sensitivity

ECR reagent and CTMAB solution flow rate effects were studied, by injecting various concentration of standard iron solution (0.1-0.3 mg $L^{-1}$) in to the flow system as shown in Figure 2.1. The total flow rate of is varied in the range 1.0 to 5.5 ml $min^{-1}$. The effect of flow rate on the sensitivity was measured as shown in Table 3.7 and Figure 3.9. It can be seen that the optimum flow rates for the carrier and reagent solutions were 4.5 ml $min^{-1}$ because at the flow rate lower than 4.5 ml $min^{-1}$, it causes higher dispersion due to band broadening. Consequently, the sensitivity was lower, when the flow rate was higher than 4.5 ml $min^{-1}$ and the reaction time was reduced. This resulted in less complex formation. Hence, the sensitivity was lower.

**Table 3.7** Effect of flow rate on the sensitivity.

| Flow rate (mL $min^{-1}$) | ΔP.H.* (AU) obtained from the standard Fe(III) (mg $L^{-1}$) | | | | | y = mx + c | $r^2$ |
|---|---|---|---|---|---|---|---|
| | 0.1 | 0.15 | 0.2 | 0.25 | 0.3 | | |
| 1.0 | 0.012 | 0.019 | 0.026 | 0.035 | 0.043 | y = 0.1580x - 0.0044 | 0.9978 |
| 1.5 | 0.018 | 0.028 | 0.036 | 0.045 | 0.053 | y = 0.1753x + 0.0009 | 0.9980 |
| 2.0 | 0.025 | 0.037 | 0.049 | 0.058 | 0.071 | y = 0.2260x + 0.0028 | 0.9976 |
| 2.5 | 0.023 | 0.039 | 0.053 | 0.065 | 0.080 | y = 0.2813x - 0.0042 | 0.9980 |
| 3.0 | 0.022 | 0.041 | 0.055 | 0.070 | 0.087 | y = 0.3180x - 0.0086 | 0.9977 |
| 3.5 | 0.026 | 0.043 | 0.061 | 0.077 | 0.096 | y = 0.3480x - 0.0090 | 0.9995 |
| 4.0 | 0.029 | 0.048 | 0.067 | 0.086 | 0.101 | y = 0.3647x - 0.0069 | 0.9982 |
| 4.5 | 0.031 | 0.051 | 0.071 | 0.090 | 0.111 | y = 0.3960x - 0.0084 | 0.9998 |
| 5.0 | 0.035 | 0.054 | 0.070 | 0.091 | 0.107 | y = 0.3607x - 0.0008 | 0.9983 |
| 5.5 | 0.035 | 0.050 | 0.069 | 0.087 | 0.107 | y = 0.3593x - 0.0023 | 0.9982 |

* average of triplicate results

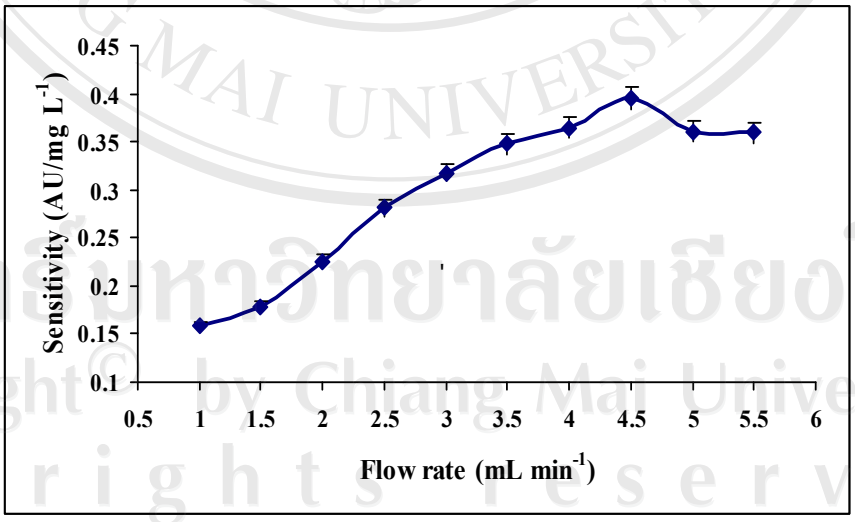


**Figure 3.9** Relationship between flow rate and sensitivity of the calibration curve.

### 3.2.1.6 Effect of reaction coil length on sensitivity

The effect of reaction coil length on the determination of Fe (III) (0.1- 0.3 mg $L^{-1}$) was studied by using Tygon tubing with diameter of 1.07 mm i.d. and lengths of reaction coil were varied from 25 to 125 cm. The results are shown in Table 3.8 and Figure 3.10. The sensitivity increased to a maximum at a reaction coil length of 75 cm give rise to an increase in the residence time allowing well mixing between iron, ECR and CTMAB. On the other hand, the sensitivity of the method decreased when the reaction coil length was beyond 75 cm. This is due to dispersion occurred when the reaction coil length exceeded 75 cm. The reaction coil length 75 cm was chosen as optimum since it provided the greatest sensitivity.

**Table 3.8** Effect of reaction coil length on the sensitivity.

| **Reaction coil length (cm)** | **ΔP.H.* (AU) obtained from the standard Fe(III) (mg $L^{-1}$)** | | | | | **y = mx + c** | **$r^2$** |
|---|---|---|---|---|---|---|---|
| | **0.1** | **0.15** | **0.2** | **0.25** | **0.3** | | |
| 25 | 0.035 | 0.050 | 0.070 | 0.088 | 0.115 | y = 0.3953x - 0.0073 | 0.9897 |
| 50 | 0.038 | 0.053 | 0.076 | 0.101 | 0.117 | y = 0.4107x - 0.0051 | 0.9923 |
| 75 | 0.038 | 0.064 | 0.084 | 0.107 | 0.127 | y = 0.4433x - 0.0047 | 0.9981 |
| 100 | 0.036 | 0.058 | 0.072 | 0.092 | 0.109 | y = 0.3593x + 0.0015 | 0.9973 |
| 125 | 0.037 | 0.056 | 0.070 | 0.087 | 0.107 | y = 0.3420x + 0.0030 | 0.9981 |

*average of triplicate results

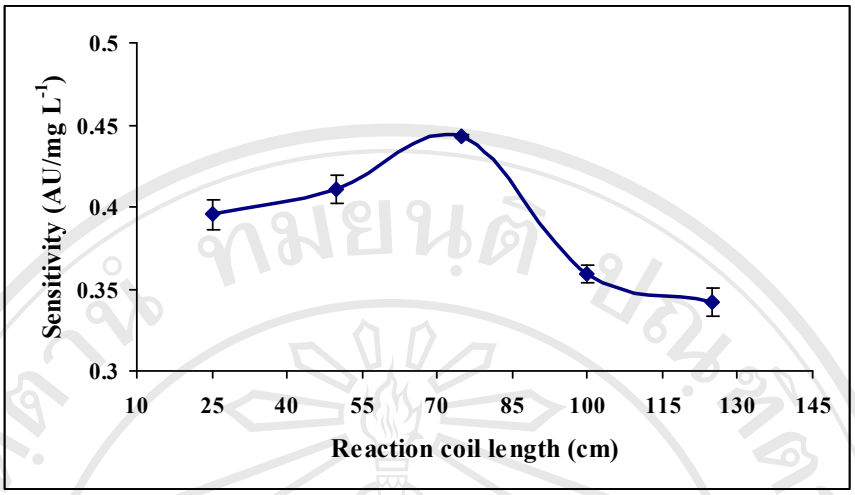


**Figure 3.10** Relationship between reaction coil length and sensitivity of the calibration curve.

### 3.2.1.7 Effect of sample volume on sensitivity

The 1.07 mm i.d. Tygon tubing was examined for making as sample loops with varying sample volumes. The sample volume injected into the reagent stream has a significant effect on the peak height. The effect of sample volume on the determination of 0.1-0.30 mg $L^{-1}$ Fe (III) was studied by varying sample volumes of 100, 150, 200, 250, 300, 350 and 400 µL. As shown in Table 3.9 and Figures 3.11, the sensitivity increases with increasing sample volume up to 250 µL. Since, the increasing of sample volume leading to increases in the number of mole of Fe (III) that causes higher absorbance. A sample volume of 250 µL was chosen as a compromise between good sensitivity, sample consumption.

**Table 3.9** Effect of sample volume on the sensitivity.

| Sample volume (µL) | ΔP.H.* (AU) obtained from the standard Fe(III) (mg $L^{-1}$) | | | | | y = mx + c | $r^2$ |
|---|---|---|---|---|---|---|---|
| | 0.1 | 0.15 | 0.2 | 0.25 | 0.3 | | |
| 100 | 0.037 | 0.057 | 0.071 | 0.094 | 0.111 | y = 0.3693x + 7E-05 | 0.9951 |
| 150 | 0.040 | 0.065 | 0.082 | 0.101 | 0.130 | y = 0.4307x - 0.0025 | 0.9916 |
| 200 | 0.050 | 0.076 | 0.103 | 0.120 | 0.140 | y = 0.4473x + 0.0083 | 0.9920 |
| 250 | 0.054 | 0.078 | 0.102 | 0.131 | 0.154 | y = 0.5073x + 0.0023 | 0.9988 |
| 300 | 0.052 | 0.080 | 0.099 | 0.123 | 0.153 | y = 0.4907x + 0.0033 | 0.9957 |
| 350 | 0.049 | 0.076 | 0.098 | 0.122 | 0.149 | y = 0.4900x + 0.0008 | 0.9987 |
| 400 | 0.049 | 0.075 | 0.096 | 0.122 | 0.144 | y = 0.4747x + 0.0023 | 0.9991 |

*average of triplicate results

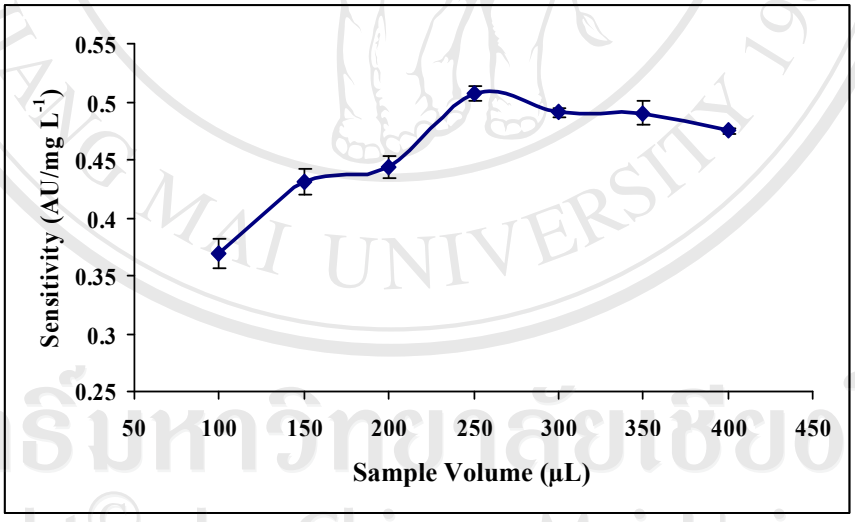


**Figure 3.11** Relationship between sample volume and sensitivity of the calibration curve.

#### 3.2.1.8 Summary of the Studied Range and Optimum Conditions

A diagram of the recommended FIA manifold is displayed in Figure 2.1. Table 3.10 shows the ranges over which the variables involved in the FIA system were studied and their optimum values.

**Table 3.10** Univariate optimization of chemical and FIA variables.

| Variable | Studied range | Optimum value |
|---|---|---|
| Wavelength (nm) | 595-625 | 610 |
| pH | 3.5-7.5 | 4.5 |
| Concentration of ECR ( x $10^{-4}$ mol $L^{-1}$) | 1.0-5.0 | 3.0 |
| Concentration of CTMAB ( x $10^{-3}$ mol $L^{-1}$) | 0.1-3.5 | 1.0 |
| Flow rate (mL $min^{-1}$) | 1.0-5.5 | 4.5 |
| Reaction Coil (cm) | 25-125 | 75 |
| Sample volume (μL) | 100-400 | 250 |

### 3.2.2 Analytical Characteristics of the method

#### 3.2.2.1 Linear range

Using the FIA manifold (Figure 2.1) and the optimum conditions in Table 3.10, linear range of calibration graph was obtained from the results for several iron standards in the concentration ranging from 0-1.50 mg $L^{-1}$. All measurements were made in pentaplicate injections. The results obtained are shown in Table 3.11 and Figure 3.12.

**Table 3.11** Peak height at various iron concentrations for linearity check of the calibration graph.

| Iron | Peak height (AU) | | | | | | ΔP.H.* |
|---|---|---|---|---|---|---|---|
| (mg $L^{-1}$) | 1 | 2 | 3 | 4 | 5 | $\bar{x}$ | (AU) |
| 0 | 0.018 | 0.017 | 0.016 | 0.016 | 0.017 | 0.017 | 0 |
| 0.01 | 0.029 | 0.027 | 0.029 | 0.028 | 0.029 | 0.028 | 0.011 |
| 0.02 | 0.032 | 0.032 | 0.032 | 0.031 | 0.032 | 0.032 | 0.015 |
| 0.03 | 0.038 | 0.037 | 0.036 | 0.039 | 0.037 | 0.037 | 0.020 |
| 0.04 | 0.041 | 0.040 | 0.043 | 0.040 | 0.043 | 0.041 | 0.024 |
| 0.05 | 0.047 | 0.046 | 0.049 | 0.048 | 0.049 | 0.048 | 0.031 |
| 0.06 | 0.053 | 0.052 | 0.050 | 0.050 | 0.054 | 0.052 | 0.035 |
| 0.07 | 0.056 | 0.056 | 0.057 | 0.057 | 0.056 | 0.056 | 0.039 |
| 0.08 | 0.065 | 0.064 | 0.066 | 0.066 | 0.066 | 0.065 | 0.048 |
| 0.09 | 0.072 | 0.071 | 0.070 | 0.071 | 0.072 | 0.071 | 0.054 |
| 0.10 | 0.075 | 0.076 | 0.075 | 0.075 | 0.073 | 0.075 | 0.058 |
| 0.11 | 0.081 | 0.083 | 0.083 | 0.082 | 0.080 | 0.082 | 0.065 |
| 0.13 | 0.092 | 0.092 | 0.093 | 0.090 | 0.092 | 0.092 | 0.075 |
| 0.15 | 0.106 | 0.104 | 0.103 | 0.104 | 0.106 | 0.105 | 0.088 |
| 0.20 | 0.132 | 0.133 | 0.134 | 0.130 | 0.132 | 0.132 | 0.115 |
| 0.25 | 0.156 | 0.157 | 0.157 | 0.157 | 0.158 | 0.157 | 0.140 |
| 0.30 | 0.184 | 0.186 | 0.185 | 0.186 | 0.186 | 0.185 | 0.168 |
| 0.35 | 0.208 | 0.208 | 0.209 | 0.208 | 0.210 | 0.209 | 0.192 |
| 0.40 | 0.231 | 0.231 | 0.231 | 0.232 | 0.232 | 0.231 | 0.214 |
| 0.45 | 0.253 | 0.253 | 0.253 | 0.255 | 0.255 | 0.254 | 0.237 |
| 0.50 | 0.290 | 0.293 | 0.290 | 0.294 | 0.292 | 0.292 | 0.275 |
| 0.55 | 0.316 | 0.316 | 0.317 | 0.316 | 0.317 | 0.316 | 0.299 |
| 0.60 | 0.336 | 0.336 | 0.335 | 0.336 | 0.335 | 0.336 | 0.319 |

**Table 3.11** (Continued).

| Iron | Peak height (AU) | | | | | | ΔP.H.* |
|---|---|---|---|---|---|---|---|
| (mg $L^{-1}$) | 1 | 2 | 3 | 4 | 5 | $\bar{x}$ | (AU) |
| 0.65 | 0.356 | 0.355 | 0.356 | 0.357 | 0.356 | 0.356 | 0.339 |
| 0.70 | 0.372 | 0.373 | 0.373 | 0.375 | 0.374 | 0.373 | 0.356 |
| 0.75 | 0.394 | 0.395 | 0.393 | 0.396 | 0.393 | 0.394 | 0.377 |
| 0.80 | 0.415 | 0.416 | 0.416 | 0.414 | 0.416 | 0.416 | 0.399 |
| 0.85 | 0.434 | 0.435 | 0.431 | 0.434 | 0.431 | 0.433 | 0.416 |
| 0.90 | 0.448 | 0.446 | 0.445 | 0.446 | 0.448 | 0.447 | 0.430 |
| 0.95 | 0.465 | 0.463 | 0.465 | 0.465 | 0.463 | 0.464 | 0.447 |
| 1.00 | 0.472 | 0.472 | 0.474 | 0.475 | 0.470 | 0.473 | 0.456 |
| 1.30 | 0.576 | 0.577 | 0.576 | 0.578 | 0.579 | 0.577 | 0.560 |
| 1.50 | 0.609 | 0.606 | 0.609 | 0.608 | 0.606 | 0.608 | 0.591 |

*average of pentaplicate results

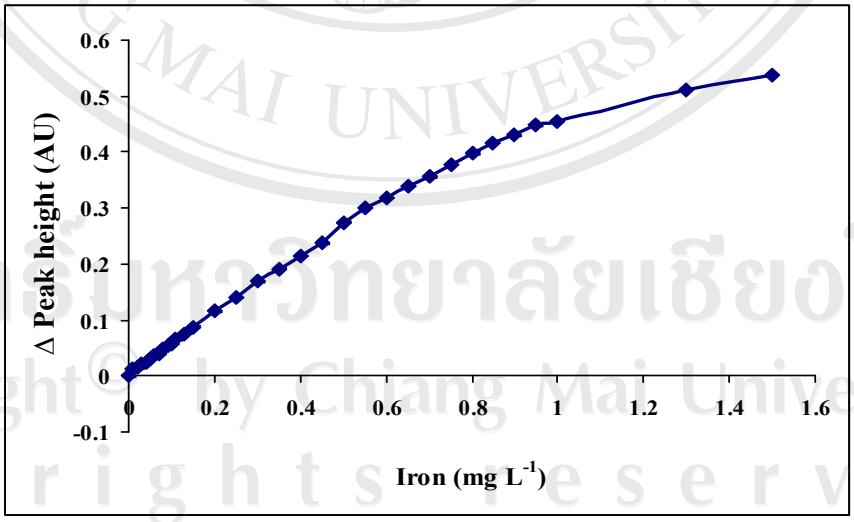


**Figure 3.12** Relationship between net peak height and concentration of iron.

### 3.2.2.2 Calibration curve

A calibration curve was obtained by injecting iron standard solutions into the recommended FIA manifold (Figure 2.1) under the optimum conditions. These results are shown in Table 3.12 and Figure 3.13-3.14. It was shown that the two linear calibration curves over the range of 0.01-0.35 mg $L^{-1}$ and 0.50-0.80 mg $L^{-1}$ with different slopes could be established. Over these two concentration ranges, linear regression analysis of iron as Fe: ECR: CTMAB peak height (y) versus iron concentration (x) (n= 8 and 7 respectively) yield the following equations:

$Y = 0.5385x + 0.0056$ ($r^2 = 0.9994$) (Fe (III) 0.01-0.35 mg $L^{-1}$)

$Y = 0.403x + 0.0759$ ($r^2 = 0.9986$) (Fe (III) 0.5-0.8 mg $L^{-1}$)

Where: y = Δpeak height in Absorbance (AU)

x = concentration of iron in mg $L^{-1}$

**Table 3.12** Peak height for calibration curve.

| Iron ($mg\ L^{-1}$) | Peak height (AU) | | | | | | ΔP.H.* (AU) |
|---|---|---|---|---|---|---|---|
| | 1 | 2 | 3 | 4 | 5 | $\bar{x}$ | |
| 0 | 0.018 | 0.017 | 0.016 | 0.016 | 0.017 | 0.017 | 0.000 |
| 0.01 | 0.029 | 0.027 | 0.029 | 0.028 | 0.029 | 0.028 | 0.011 |
| 0.05 | 0.047 | 0.046 | 0.049 | 0.048 | 0.049 | 0.048 | 0.031 |
| 0.10 | 0.075 | 0.076 | 0.075 | 0.075 | 0.073 | 0.075 | 0.058 |
| 0.15 | 0.106 | 0.104 | 0.103 | 0.104 | 0.106 | 0.105 | 0.088 |
| 0.20 | 0.132 | 0.133 | 0.134 | 0.130 | 0.132 | 0.132 | 0.115 |
| 0.25 | 0.156 | 0.157 | 0.157 | 0.157 | 0.158 | 0.157 | 0.140 |
| 0.30 | 0.184 | 0.186 | 0.185 | 0.186 | 0.186 | 0.185 | 0.168 |
| 0.35 | 0.208 | 0.208 | 0.209 | 0.208 | 0.210 | 0.209 | 0.192 |
| 0.50 | 0.290 | 0.293 | 0.290 | 0.294 | 0.292 | 0.292 | 0.275 |
| 0.55 | 0.316 | 0.316 | 0.317 | 0.316 | 0.317 | 0.316 | 0.299 |
| 0.60 | 0.336 | 0.336 | 0.335 | 0.336 | 0.335 | 0.336 | 0.319 |
| 0.65 | 0.356 | 0.355 | 0.356 | 0.357 | 0.356 | 0.356 | 0.339 |
| 0.70 | 0.372 | 0.373 | 0.373 | 0.375 | 0.374 | 0.373 | 0.356 |
| 0.75 | 0.394 | 0.395 | 0.393 | 0.396 | 0.393 | 0.394 | 0.377 |
| 0.80 | 0.415 | 0.416 | 0.416 | 0.414 | 0.416 | 0.416 | 0.399 |

*average of pentaplicate results

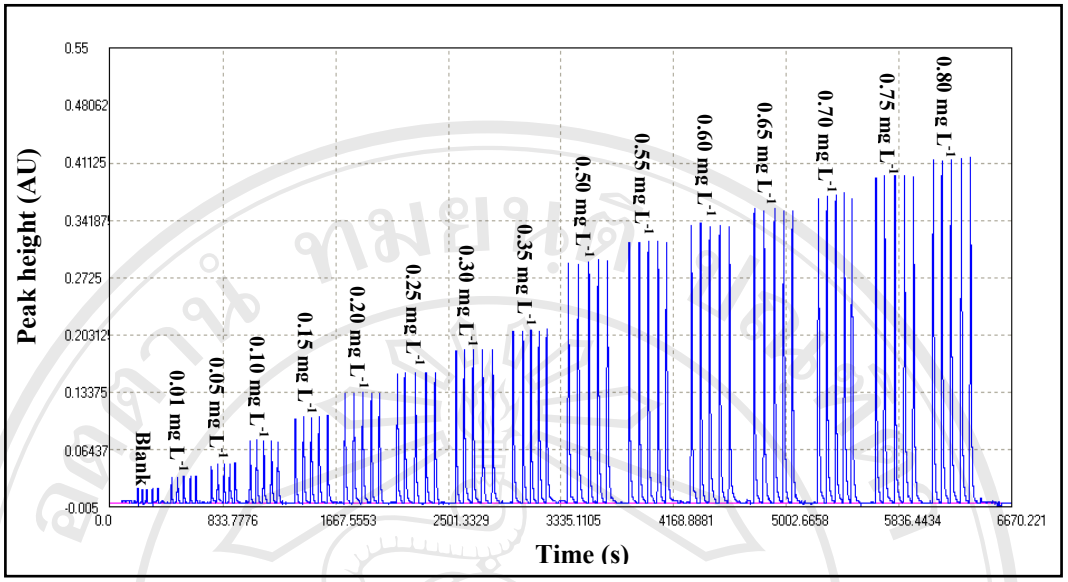


**Figure 3.13** Calibration signal of FIA spectrophotometric determination of iron 0.01-0.35 mg $L^{-1}$ and 0.50–0.80 mg $L^{-1}$.

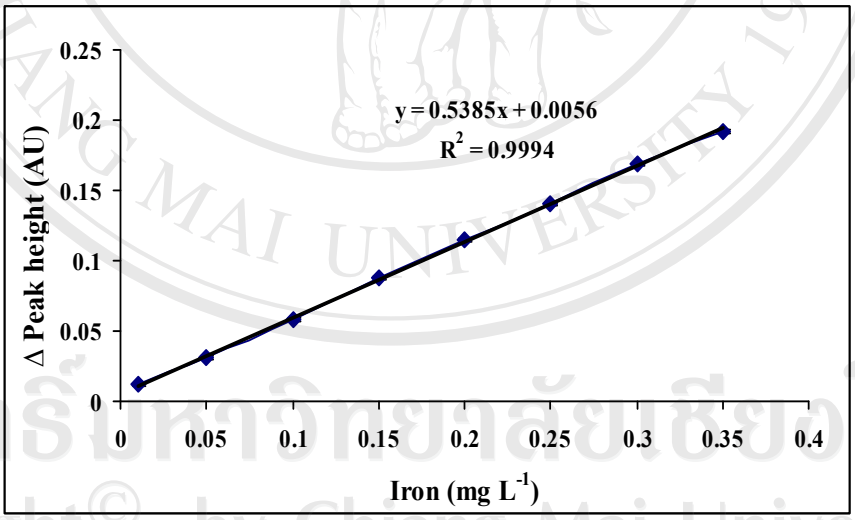


(a)

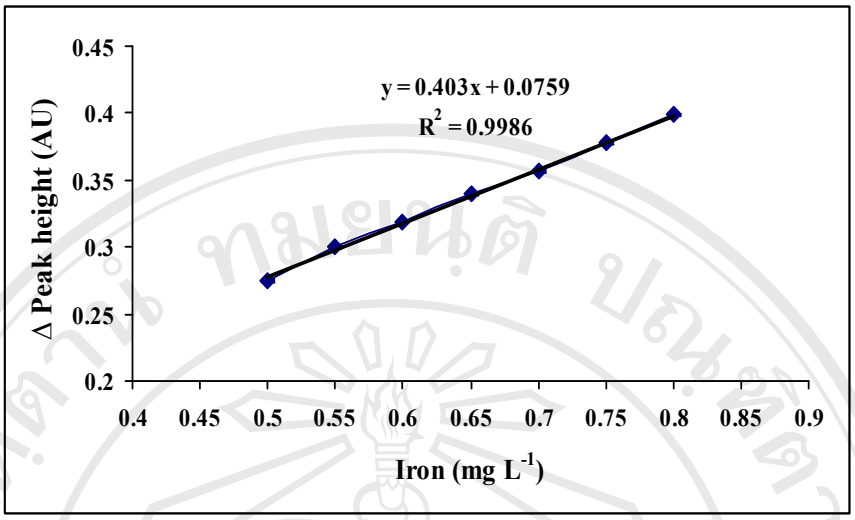


(b)

**Figure 3.14** The calibration curve of FIA spectrophotometric determination of iron (III): (a) iron 0.01-0.35 mg $L^{-1}$; (b) iron 0.50–0.80 mg $L^{-1}$.

### 3.2.2.3 Precision of the flow injection system

The precision of the proposed method was verified by injecting 11 replicates of 0.1 mg $L^{-1}$ standard iron, using the optimum conditions in Table 3.10. The results were shown in Table 3.13. The relative standard deviation was found to be 1.19%.

**Table 3.13** Precision of verification using standard 0.1 mg $L^{-1}$ iron.

| Experimental number | Peak height (AU)* |
|---|---|
| 1 | 0.059 |
| 2 | 0.059 |
| 3 | 0.060 |
| 4 | 0.058 |
| 5 | 0.060 |
| 6 | 0.058 |
| 7 | 0.059 |
| 8 | 0.060 |
| 9 | 0.059 |
| 10 | 0.058 |
| 11 | 0.059 |
| $\overline{X}$ | 0.059 |
| S.D. | 0.0007 |
| % R.S.D. | 1.19 |

*average of triplicate results

#### 3.2.2.4 Detection limit

The detection limits is defined as that concentration of the analyte producing a signal (peak height) which is the experimental blank signal plus three times of the standard deviation of the blank signal [67]. Using the FIA manifold (Figure 2.1) and the optimum conditions in Table 3.10. The detection limit of the proposed method was found to be 0.005 mg $L^{-1}$.

**Table 3.14** The blank signal resulting from 12 injections.

| Experimental number | Peak height (AU) * |
|---|---|
| 1 | 0.018 |
| 2 | 0.017 |
| 3 | 0.018 |
| 4 | 0.020 |
| 5 | 0.018 |
| 6 | 0.018 |
| 7 | 0.017 |
| 8 | 0.019 |
| 9 | 0.019 |
| 10 | 0.018 |
| 11 | 0.018 |
| 12 | 0.020 |
| $\overline{X}$ | 0.018 |
| S.D. | 0.0009 |
| LOD (mg $L^{-1}$) | 0.005 |

*average of triplicate results

**3.2.2.5 Interferences Studies**

The effects of some possible interfering ions on the determination of 0.1 mg $L^{-1}$ iron were studied for the maximum w/w ratio of interfering ions to iron up to 1000:1. The tolerance value (defined as the foreign-ion concentration causing an error smaller than ±10% for determining the analyte of interest) for the ions studied are listed in Table 3.15. Most ions studied do not interfere with the determination of iron (III). Among the interfering cations studied aluminum and iron (II) exhibited rather serous effect on iron (III) determination. It led to the enhancement of FI signals,

probably due to the formation of complexes with ECR which absorb at the same or very near to the working wavelength, however the concentration of iron (II) in drinking water is very low and it can be eliminated by adding 30% $H_2O_2$ solution [54]. Al (III) was masked with NaF [69].

**Table 3.15** Effect of interference study for 0.1 mg $L^{-1}$ standard iron.

| **Ions** | **Chemical form added** | **Concentration added (mg $L^{-1}$)** | **Peak height (AU)*** | **% Relative Error** |
|---|---|---|---|---|
| none | - | - | 0.059 | - |
| $Al^{3+}$ | $Al(NO_3)_2$ | 0.1 | 0.063 | +5.39 |
| | | 0.2 | 0.065 | +9.42 |
| | | 0.3 | 0.067 | +12.12 |
| | | 0.4 | 0.069 | +16.16 |
| | | 0.5 | 0.074 | +25.25 |
| $Fe^{2+}$ | $FeSO_4$ | 0.05 | 0.062 | +5.05 |
| | | 0.1 | 0.065 | +9.76 |
| | | 0.2 | 0.067 | +12.50 |
| | | 0.3 | 0.068 | +14.50 |
| | | 0.4 | 0.070 | +17.80 |
| $Ca^{2+}$ | $Ca(NO_3)_2$ | 100 | 0.056 | -5.39 |
| | | 300 | 0.056 | -5.39 |
| | | 500 | 0.055 | -7.41 |
| | | 800 | 0.054 | -9.43 |
| | | 1000 | 0.052 | -12.78 |
| $Cu^{2+}$ | $Cu(NO_3)_2$ | 10 | 0.061 | +3.37 |
| | | 15 | 0.064 | +8.42 |
| | | 20 | 0.067 | +13.47 |
| | | 25 | 0.070 | +17.84 |
| | | 30 | 0.074 | +24.24 |

**Table 3.15** (Continued).

| Ions | Chemical form added | Concentration added (mg $L^{-1}$) | Peak height (Abs.)* | % Relative Error |
|---|---|---|---|---|
| none | - | - | 0.059 | - |
| $Co^{2+}$ | $Co(NO_3)_2$ | 100 | 0.0576 | -0.34 |
| | | 200 | 0.0564 | -1.35 |
| | | 300 | 0.0554 | -5.72 |
| | | 600 | 0.0544 | -9.43 |
| | | 900 | 0.0514 | -11.78 |
| $Cr^{3+}$ | $Cr(NO_3)_2$ | 10 | 0.062 | +4.04 |
| | | 15 | 0.064 | +8.08 |
| | | 30 | 0.065 | +9.76 |
| | | 40 | 0.065 | +9.76 |
| | | 50 | 0.066 | +11.11 |
| $Mn^{2+}$ | $Mg(NO_3)_2$ | 100 | 0.060 | +1.68 |
| | | 200 | 0.062 | +4.04 |
| | | 300 | 0.064 | +7.74 |
| | | 400 | 0.065 | +9.43 |
| | | 500 | 0.067 | +12.12 |
| $Mg^{2+}$ | $Mg(NO_3)_2$ | 300 | 0.058 | -2.02 |
| | | 500 | 0.057 | -4.71 |
| | | 700 | 0.055 | -7.07 |
| | | 900 | 0.055 | -8.08 |
| | | 1000 | 0.053 | -10.77 |
| $Na^{+}$ | $NaNO_3$ | 100 | 0.059 | 0 |
| | | 300 | 0.057 | -4.04 |
| | | 500 | 0.055 | -7.74 |
| | | 800 | 0.052 | -11.78 |
| | | 1000 | 0.051 | -14.81 |

**Table 3.15** (Continued).

| Ions | Chemical form added | Concentration added (mg $L^{-1}$) | Peak height (AU)* | % Relative Error |
|---|---|---|---|---|
| none | - | - | 0.059 | - |
| $Ni^{2+}$ | $Ni(NO_3)_2$ | 50 | 0.059 | 0 |
| | | 100 | 0.058 | -3.03 |
| | | 200 | 0.056 | -5.39 |
| | | 300 | 0.054 | -8.42 |
| | | 600 | 0.051 | -14.81 |
| $Zn^{2+}$ | $Zn(NO_3)_2$ | 100 | 0.057 | -3.70 |
| | | 200 | 0.056 | -5.72 |
| | | 300 | 0.054 | -9.43 |
| | | 400 | 0.050 | -15.49 |
| | | 500 | 0.049 | -17.51 |
| $Br^-$ | NaBr | 100 | 0.059 | 0 |
| | | 300 | 0.059 | 0 |
| | | 500 | 0.059 | 0 |
| | | 800 | 0.057 | -3.70 |
| | | 1000 | 0.055 | -7.74 |
| $Cl^-$ | NaCl | 100 | 0.059 | 0 |
| | | 300 | 0.059 | 0 |
| | | 500 | 0.059 | 0 |
| | | 800 | 0.059 | 0 |
| | | 1000 | 0.060 | +1.01 |
| $HCO_3^-$ | $NaHCO_3$ | 50 | 0.059 | 0 |
| | | 100 | 0.055 | -8.08 |
| | | 150 | 0.054 | -9.76 |
| | | 200 | 0.052 | -12.46 |
| | | 300 | 0.0474 | -20.20 |

**Table 3.15** (Continued).

| Ions | Chemical form added | Concentration added (mg $L^{-1}$) | Peak height (AU)* | % Relative Error |
|---|---|---|---|---|
| none | - | - | 0.059 | - |
| $I^-$ | NaI | 5 | 0.056 | -5.72 |
| | | 10 | 0.055 | -7.74 |
| | | 20 | 0.054 | -9.43 |
| | | 30 | 0.050 | -16.49 |
| | | 40 | 0.045 | -24.24 |
| $NO_2^-$ | $NaNO_2$ | 5 | 0.061 | +2.36 |
| | | 10 | 0.062 | +4.38 |
| | | 15 | 0.064 | +7.41 |
| | | 20 | 0.065 | +9.76 |
| | | 30 | 0.066 | +11.11 |
| $NO_3^-$ | $NaNO_3$ | 100 | 0.059 | 0 |
| | | 300 | 0.057 | -3.70 |
| | | 500 | 0.056 | -5.72 |
| | | 800 | 0.055 | -7.41 |
| | | 1000 | 0.054 | -9.76 |
| $PO_4^{3-}$ | $Na_3PO_4 \cdot 12H_2O$ | 200 | 0.059 | -1.35 |
| | | 300 | 0.058 | -3.03 |
| | | 330 | 0.057 | -5.05 |
| | | 350 | 0.054 | -9.09 |
| | | 370 | 0.049 | -18.18 |
| $SO_4^{2-}$ | $Na_2SO_4$ | 100 | 0.060 | +1.01 |
| | | 300 | 0.061 | +3.03 |
| | | 500 | 0.063 | +5.72 |
| | | 800 | 0.064 | +8.08 |
| | | 1000 | 0.065 | +9.09 |

*average of triplicate results

The interference effects of some possible foreign ions in the FIA system for iron were summarized in Table 3.16. It was found $Al^{3+}$ interfered iron determination in bottled-drinking water, which referred standard quality of bottled-drinking water defined by pollution control department, ministry of natural resources and environment (WHO 2006) [72]. (Appendix A). So, aluminum in the water samples was eliminated by the addition of sodium fluoride as the masking agent [69].

**Table 3.16** Summary of the interference effects of some ions on the responses obtains from 0.1 mg $L^{-1}$ Fe (III).

| **Interference ions** | **Tolerable concentration ratio* (mg $L^{-1}$) of ion/Fe (III)** |
|---|---|
| $Br^-$, $Cl^-$, $SO_4^{2-}$, $NO_3^-$, | ≥1000 |
| $Mg^{2+}$ | 900 |
| $Ca^{2+}$ | 800 |
| $Co^{2+}$ | 600 |
| $Na^+$ | 500 |
| $Mn^{2+}$ | 400 |
| $PO_4^{3-}$ | 350 |
| $Ni^{2+}$, $Zn^{2+}$ | 300 |
| $HCO_3^-$, $I^-$ | 150 |
| $Cr^{3+}$ | 40 |
| $NO_2^-$ | 20 |
| $Cu^{2+}$ | 15 |
| $Fe^{2+}$, $Al^{3+}$ | <1 |

*The concentration of an ion is considered to be interfering when causing a relative error of more than ±10% with respect to the signal of Fe (III) alone.

### 3.2.2.6 Effect of masking agents for the removal of Al (III) interference

The effect of masking agent and interference was studied by the proposed FIA procedure under the optimum conditions. In order to reduce interference effects of $Al^{3+}$. A concentration of NaF as masking agent for Fe (III) determination was investigated. The results are shown in Table 3.17. The result indicated that at 0.0006 mol $L^{-1}$ of sodium fluoride is the optimum concentration which does not affect the sensitivity. The interference from aluminum up to 1.5 mg $L^{-1}$ was completely removed by adding 0.0006 mol $L^{-1}$ sodium fluoride.

**Table 3.17** Effect of masking agent for $Al^{3+}$ the response obtained from Fe (III) (0.1 mg $L^{-1}$).

| Interference | Concentration of masking agent | Iron : Interference | Peak height (AU) | % Relative Error |
|---|---|---|---|---|
| $Al^{3+}$ | 0.0004 mol $L^{-1}$ $F^-$ | 1:0 | 0.059 | - |
| | | 1:1 | 0.060 | +3.03 |
| | | 1:5 | 0.062 | +4.71 |
| | | 1:10 | 0.064 | +8.08 |
| | | 1:15 | 0.066 | +11.78 |
| | | 1:20 | 0.072 | +20.87 |
| | 0.0006 mol $L^{-1}$ $F^-$ | 1:0 | 0.059 | - |
| | | 1:1 | 0.061 | +2.69 |
| | | 1:5 | 0.062 | +4.71 |
| | | 1:10 | 0.064 | +7.07 |
| | | 1:15 | 0.065 | +9.09 |
| | | 1:20 | 0.067 | +13.47 |

*average of triplicate results

**Table 3.17** (Continued).

| Interference | Concentration of masking agent | Iron : Interference | Peak height (AU) | % Relative Error |
|---|---|---|---|---|
| $Al^{3+}$ | 0.0008 mol $L^{-1}$ $F^-$ | 1:0 | 0.059 | - |
| | | 1:1 | 0.061 | +2.69 |
| | | 1:5 | 0.062 | +4.71 |
| | | 1:10 | 0.064 | +7.74 |
| | | 1:15 | 0.066 | +11.11 |
| | | 1:20 | 0.067 | +13.13 |

### 3.2.2.7 Determination of total Fe in drinking water samples

The proposed FIA spectrophotometric method was applied to the simultaneous determination of iron in drinking water samples which were commercial drinking waters available in the market around Chiang Mai Municipality. The peak heights from each sample were compared with standard calibration curve. The results were given in Table 3.18.

**Table 3.18** Determination of iron in drinking water samples by FIA method.

| Water samples brand | Peak heights | | | | SD | Iron concentration* (mg $L^{-1}$) | % recovery* |
|---|---|---|---|---|---|---|---|
| | 1 | 2 | 3 | $\overline{X}$ | | | |
| Amtech | 0.006 | 0.007 | 0.007 | 0.007 | 0.001 | 0.007 ± 0.001 | 99.57 |
| Big Bell | 0.016 | 0.015 | 0.015 | 0.015 | 0.001 | 0.015 ± 0.001 | 99.40 |
| Double Elephants | 0.013 | 0.010 | 0.008 | 0.010 | 0.003 | 0.010 ± 0.003 | 101.05 |
| F&B | ND** | ND** | ND** | - | - | ND** | - |
| Free Bird | ND** | ND** | ND** | - | - | ND** | - |
| Mont Blanc | 0.008 | 0.012 | 0.007 | 0.009 | 0.003 | 0.009 ± 0.003 | 99.57 |
| Nam Petch | 0.005 | 0.007 | 0.005 | 0.006 | 0.001 | 0.006 ± 0.001 | 102.29 |
| Nasibee | 0.017 | 0.016 | 0.015 | 0.016 | 0.001 | 0.016 ± 0.001 | 99.33 |
| Pola | ND** | ND** | ND** | - | - | ND** | - |
| Polestar | 0.006 | 0.006 | 0.007 | 0.006 | 0.001 | 0.006 ± 0.001 | 101.28 |
| Rintip | ND** | ND** | ND** | - | - | ND** | - |
| Wang Nam Kang | 0.008 | 0.007 | 0.010 | 0.008 | 0.002 | 0.008 ± 0.002 | 102.16 |

*average of triplicate results

**not detected

The iron (III) contents in drinking water samples were in the range 0.006-0.016 mg $L^{-1}$ and <0.0005-0.018 mg $L^{-1}$ using the proposed method and ICP-MS (Agilent 7500 C) respectively. The results obtained by the proposed FI spectrophotometric method compared with those obtained by ICP-MS using the student *t*-test (Table 3.19) and Appendix B in Table B.1). It was evident that the *t*-value for Fe (III) contents in drinking water samples determined by comparison the results obtained by FI spectrophotometric with those obtained by ICP-MS were -1.001, -5.004, -1.811,

-0.218, -0.499, -3.464, -1.633 and -1.891, for samples Amtech, Big Bell, Double Elephants, Mont Blanc, Nam Petch Nasibee, Polestar and Wang Nam Kang, respectively. It was seen that experimental *t*-value for Fe(III) assay, which was smaller than the theoretical *t*-value at a confidence interval of 95% (4.30) indicating that results obtained by both methods were in excellent agreement.

**Table 3.19** Comparative determination of iron in drinking water samples by proposed FIA and ICP-MS.

| **Drinking water sample** | **Concentrations (mg $L^{-1}$)** | | $t_{calculated}$ |
|---|---|---|---|
| | **FIA*** | **ICP-MS*** | |
| Amtech | 0.007 | 0.007 | -1.001 |
| Big Bell | 0.015 | 0.017 | -5.004 |
| Double Elephants | 0.010 | 0.013 | -1.811 |
| F&B | ND** | <0.0005 | - |
| Free Bird | ND** | <0.0005 | - |
| Mont Blanc | 0.009 | 0.010 | -0.218 |
| Nam Petch | 0.006 | 0.006 | -0.499 |
| Nasibee | 0.016 | 0.018 | -3.464 |
| Pola | ND** | <0.0005 | - |
| Polestar | 0.006 | 0.007 | -1.633 |
| Rrintip | ND** | <0.0005 | - |
| Wang Nam Kang | 0.008 | 0.010 | -1.891 |

*average of triplicate results

**not detected

### 3.3 SIA Spectrophotometric Determination of Iron (III) Using Eriochrome Cyanine R and Cetyltrimethyl Ammonium Bromide as A Complexing Agent

The sequential injection analysis system with spectrophotometric detection was used for iron (III) determination, manifold as shown in Figure 2.2. The optimization of the SIA and the chemical conditions were carried out by univariate method. The conditions for the determination of iron (III) was optimized by studying the influences of the various parameters such as flow rate, sample and reagent volume, reaction coil length, holding coil length and reagent concentration. All optimum values were chosen by judging from the greatest peak height, stability of the base line, low or no positive blank signal and relative standard deviation. To optimize the conditions, the preliminary experimental conditions in Table 2.5 were used. The range of variables studied and the optimal values chosen are shown in Table 2.4.

#### 3.3.1 Study aspiration order

The complexation of Fe-ECR-CTMAB was studied at different aspiration orders. The sensitivities obtained are shown in Table 3.20. It was found that the aspiration order of first series provides a highest sensitivity. So, aspiration order of first series was chosen for further optimization of SIA method.

**Table 3.20** Sensitivity at various aspiration orders.

| Series | Aspiration order | Sensitivity (AU/mg $L^{-1}$) |
|---|---|---|
| 1 | A-B-C | 0.187 |
| 2 | A-C-B | ND* |
| 3 | B-A-C | 0.154 |
| 4 | B-C-A | ND* |
| 5 | C-A-B | ND* |
| 6 | C-B-A | 0.128 |

*not detected

A was 0.1 mg $L^{-1}$ iron standard solution

B was 3.0 x $10^{-4}$ mol $L^{-1}$ Eriochrome Cyanine R

C was 1 x $10^{-3}$ mol $L^{-1}$ cetyltrimethylammonium bromide

### 3.3.2 Optimization of the sequential injection system by univariate method

To optimize the experimental conditions, the SIA manifold in Figure 2.2 and the software in Fig. 2.3 were employed and the preliminary experimental conditions (Table 2.5) were investigated.

### 3.3.2.1 Effect of pH on the sensitivity

The formation of the complexes and their stability are strongly dependent on the pH of the solution. The influence of pH on the absorbance of the Fe (III)-ECR-CTMAB complex was studied in the range of pH 4.0-6.0 in 0.1 mol $L^{-1}$ acetate buffer media. The results were shown in Table 3.21 and Figure 3.15, less colored complex of iron (III) was produced at the lowest examined pH 4.0. The sensitivity for iron (III) was maximum pH 5.5. At above pH 5.5 the sensitivity decreased. Thus, 0.1 mol $L^{-1}$ acetate buffer solution of pH 5.5 was used for determination of iron (III).

**Table 3.21** Effect of pH on the sensitivity.

| pH | Sensitivity (AU/mg $L^{-1}$) | | | | SD |
|---|---|---|---|---|---|
| | 1 | 2 | 3 | $\bar{x}$ * | |
| 4.0 | 0.102 | 0.106 | 0.108 | 0.105 | 0.0030 |
| 4.5 | 0.150 | 0.142 | 0.144 | 0.145 | 0.0042 |
| 5.0 | 0.159 | 0.164 | 0.161 | 0.161 | 0.0025 |
| 5.5 | 0.174 | 0.167 | 0.169 | 0.169 | 0.0036 |
| 6.0 | 0.139 | 0.145 | 0.144 | 0.142 | 0.0032 |

* average of triplicate results

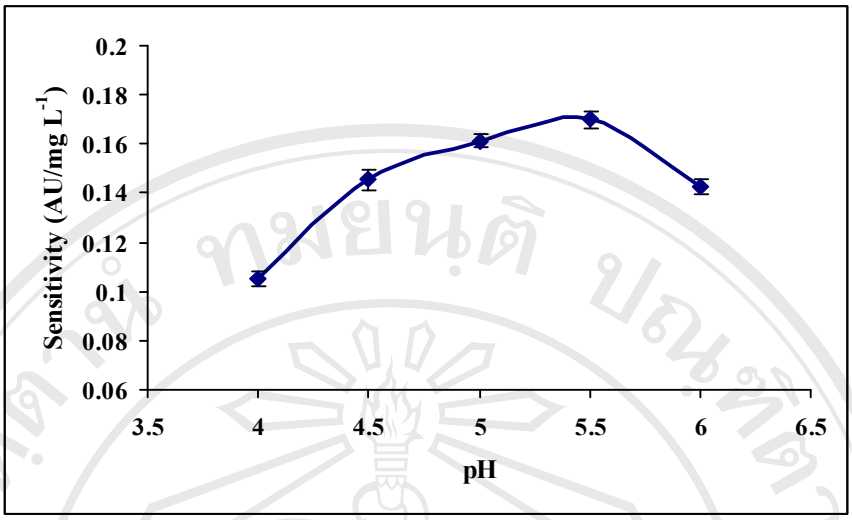


**Figure 3.15** Relationship between various pH and sensitivity of the calibration curve.

### 3.3.2.2 Effect of concentration of acetate buffer on the sensitivity

The effect of the concentration of buffer solution was investigated within the range 0.01-0.2 mol $L^{-1}$. The results are shown in Table 3.22 and Figure 3.16. It was found that the sensitivity of the SI method increased from the acetate buffer concentration of 0.01-0.1 mol $L^{-1}$. After that, the sensitivity was decreased. Therefore, 0.1 mol $L^{-1}$ of acetate solution was chosen for subsequent experiments since it gave the highest sensitivity.

**Table 3.22** Effect of concentration of acetate buffer pH 5.5 on the sensitivity.

| Concentration of acetate buffer pH 5.5 (mol $L^{-1}$) | Sensitivity (AU/mg $L^{-1}$) | | | | SD |
|---|---|---|---|---|---|
| | 1 | 2 | 3 | $\bar{x}$ * | |
| 0.01 | 0.127 | 0.119 | 0.118 | 0.121 | 0.0049 |
| 0.05 | 0.166 | 0.169 | 0.172 | 0.169 | 0.0030 |
| 0.10 | 0.185 | 0.180 | 0.176 | 0.180 | 0.0045 |
| 0.15 | 0.175 | 0.172 | 0.174 | 0.174 | 0.0015 |
| 0.20 | 0.158 | 0.145 | 0.143 | 0.148 | 0.0081 |

*average of triplicate results

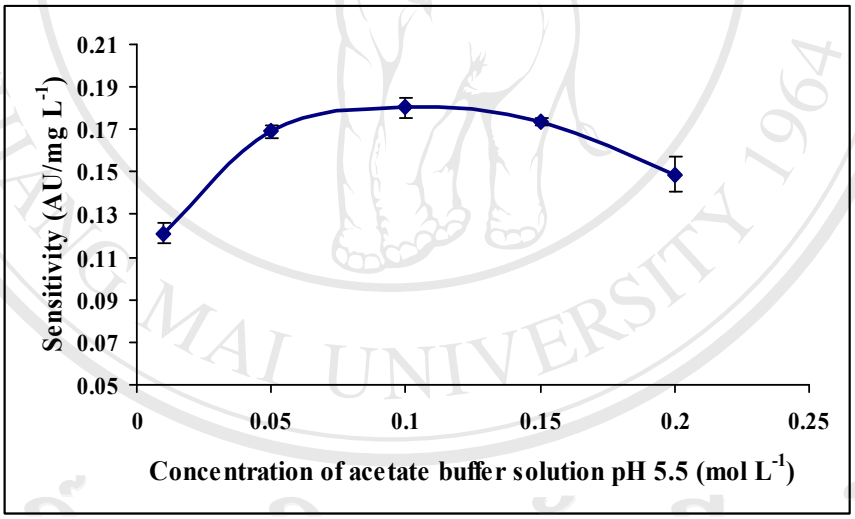


**Figure 3.16** Relationship between various concentrations of acetate buffer pH 5.5 and sensitivity of the calibration curve.

### 3.3.2.3 Effect of ECR concentration on the sensitivity

The concentration of the reagent was studied between 2.5 x $10^{-4}$ mol $L^{-1}$ and 4.5 x $10^{-4}$ mol $L^{-1}$ of ECR. As can be seen in Table 3.23 and Figure 3.17. The sensitivity increased with increasing the ECR reagent concentration up to 3.5 x $10^{-4}$ mol $L^{-1}$, above which it decreased. Thus, a concentration of 3.5 x $10^{-4}$ mol $L^{-1}$ ECR was chosen for subsequent experiments since it provided a high analytical signal.

**Table 3.23** Effect of various concentration of ECR on the sensitivity.

| **Concentration of ECR solutions ( x $10^{-4}$ mol $L^{-1}$)** | **Sensitivity (AU/mg $L^{-1}$)** | | | | **SD** |
|---|---|---|---|---|---|
| | **1** | **2** | **3** | **$\bar{x}$ *** | |
| 2.5 | 0.153 | 0.157 | 0.154 | 0.155 | 0.0021 |
| 3.0 | 0.168 | 0.162 | 0.165 | 0.165 | 0.0030 |
| 3.5 | 0.184 | 0.181 | 0.177 | 0.181 | 0.0035 |
| 4.0 | 0.148 | 0.144 | 0.142 | 0.144 | 0.0031 |
| 4.5 | 0.140 | 0.141 | 0.143 | 0.141 | 0.0015 |

*average of triplicate results

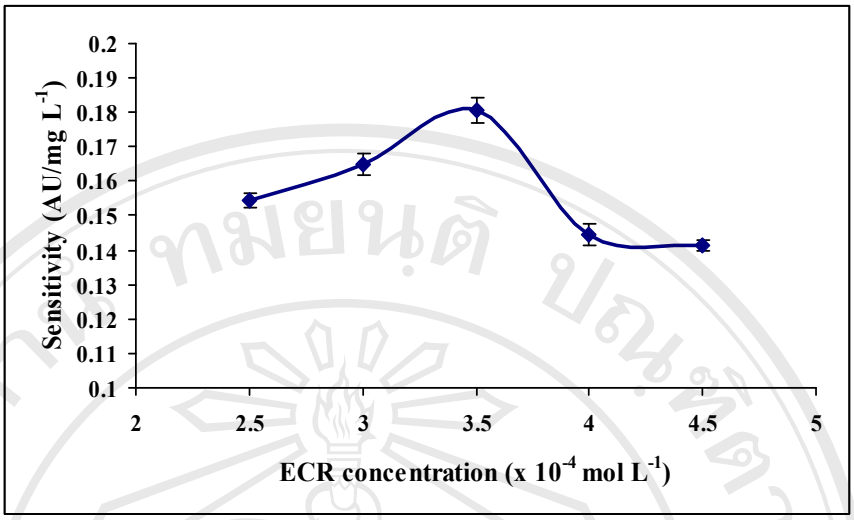


**Figure 3.17** Relationship between various concentration of ECR solution and sensitivity of the calibration curve.

### 3.3.2.4 Effect of CTMAB concentration on the sensitivity

The effect of the surfactant CTMAB concentration on the formation of Fe (III)-ECR complex was studied over the CTMAB concentration range $1.0 \times 10^{-3}$ - $3.0 \times 10^{-3}$ mol $L^{-1}$, as shown in Table 3.24 and Figure 3.18. The study revealed that maximum enhancement of the complex absorbance was obtained at a concentration of $2.5 \times 10^{-3}$ mol $L^{-1}$ CTMAB. When the concentration was more than of $2.5 \times 10^{-3}$ mol $L^{-1}$ CTMAB, the sensitivity was decreased markedly. Therefore, $2.5 \times 10^{-3}$ mol $L^{-1}$ of CTMAB was adopted for further experiments.

**Table 3.24** Effect of various concentration of CTMAB on the sensitivity.

| CTMAB of concentration ( $\times 10^{-3}$ mol $L^{-1}$) | Sensitivity (AU/mg $L^{-1}$) | | | | SD |
|---|---|---|---|---|---|
| | 1 | 2 | 3 | $\bar{x}$ * | |
| 1.0 | 0.182 | 0.174 | 0.181 | 0.179 | 0.0043 |
| 1.5 | 0.184 | 0.184 | 0.179 | 0.182 | 0.0028 |
| 2.0 | 0.184 | 0.187 | 0.186 | 0.186 | 0.0015 |
| 2.5 | 0.211 | 0.213 | 0.207 | 0.207 | 0.0030 |
| 3.0 | 0.157 | 0.155 | 0.155 | 0.156 | 0.0011 |

*average of triplicate results

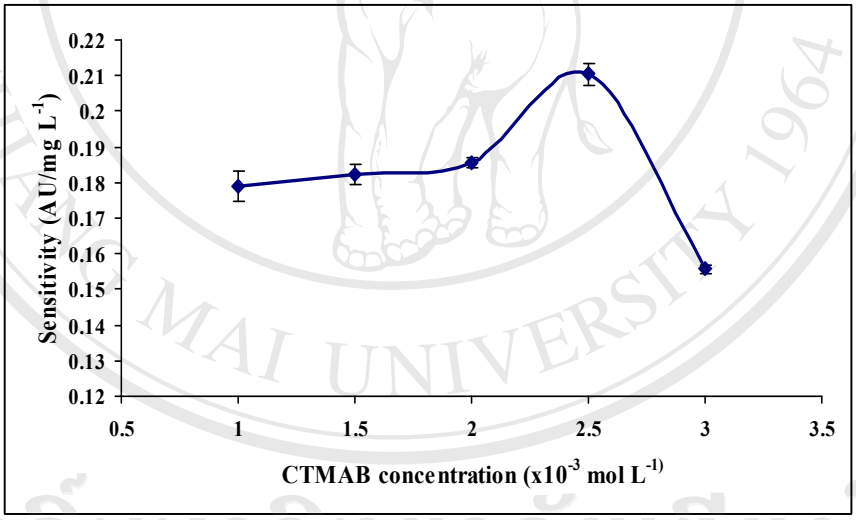


**Figure 3.18** Relationship between concentrations of CTMAB on the sensitivity of the calibration curve.

### 3.3.2.5 Effect of aspiration volumes of acetate buffer on the sensitivity

The sample and reagent solution are very important for the successful exploitation of the method. The volume supplied should be enough for an effective determination to talk place. The aim was to find the least consumption of reagent yet giving the best sensitivity and reproducibility. The pattern adopted for the optimizing of this parameter was to keep the volume of one of the reagent constant while varying the other one. For instance, the effect of aspiration volume of 0.1 mol $L^{-1}$ of acetate buffer pH 5.5 were evaluated over the range from 25-125 µL at every 25 µL interval and the results obtained are depicted in Table 3.25 and Figure 3.19. The best sensitivity was obtained with a 0.1 mol $L^{-1}$ acetate buffer pH 5.5 volumes of 50 µL and this was chosen as optimum for further work.

**Table 3.25** Effect of various aspiration volumes of 0.1 mol $L^{-1}$ of acetate buffer pH 5.5 on the sensitivity.

| **Aspiration volume of buffer (µL)** | **Sensitivity (AU/mg $L^{-1}$)** | | | | **SD** |
|---|---|---|---|---|---|
| | **1** | **2** | **3** | **$\bar{x}$ *** | |
| 25 | 0.183 | 0.185 | 0.186 | 0.185 | 0.0015 |
| 50 | 0.223 | 0.215 | 0.219 | 0.219 | 0.0040 |
| 75 | 0.193 | 0.193 | 0.191 | 0.192 | 0.0011 |
| 100 | 0.188 | 0.191 | 0.188 | 0.189 | 0.0016 |
| 125 | 0.182 | 0.180 | 0.179 | 0.180 | 0.0015 |

*average of triplicate results

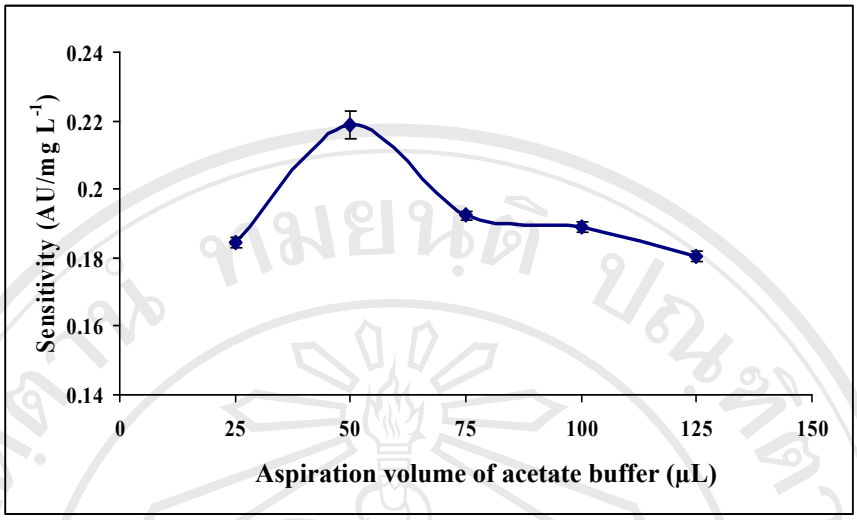


**Figure 3.19** Relationship between various aspiration volumes of 0.1 mol $L^{-1}$ of acetate buffer pH 5.5 on the sensitivity of the calibration curve.

### 3.3.2.6 Effect of aspiration volumes of ECR on the sensitivity

The effect of ECR aspiration volumes was evaluated from 100 to 200 µL and the results are given in Table 3.26 and Figure 3.20. It was found that, the sensitivity increased with increasing aspiration volumes up to 175 µL, after that the sensitivity was decreased. Smaller ECR reagent volume (125-175 µL) gave slightly better sensitivity, probably due to better zone overlap which resulted from a better dispersion of the reagent zone [71]. An aspiration volume of 175 µL ECR was selected as optimum for further work.

**Table 3.26** Effect of various aspiration volumes of $3.5\times10^{-4}$ mol $L^{-1}$ of ECR on the sensitivity.

| Aspiration volume of ECR (µL) | Sensitivity (AU/mg $L^{-1}$) | | | | SD |
|---|---|---|---|---|---|
| | 1 | 2 | 3 | $\bar{x}$* | |
| 100 | 0.163 | 0.165 | 0.165 | 0.164 | 0.0011 |
| 125 | 0.175 | 0.173 | 0.176 | 0.175 | 0.0015 |
| 150 | 0.182 | 0.179 | 0.178 | 0.180 | 0.0021 |
| 175 | 0.209 | 0.213 | 0.211 | 0.211 | 0.0020 |
| 200 | 0.167 | 0.166 | 0.162 | 0.165 | 0.0026 |
| 225 | 0.139 | 0.135 | 0.137 | 0.137 | 0.0020 |

*average of triplicate results

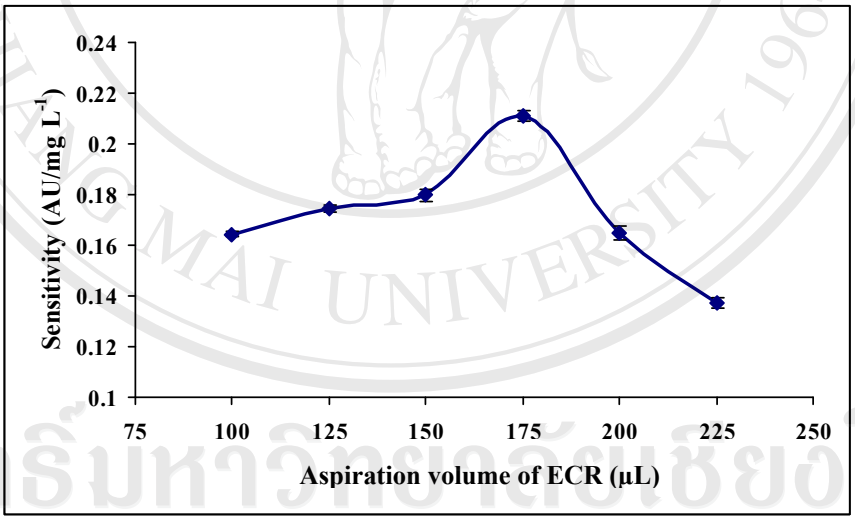


**Figure 3.20** Relationship between various aspiration volumes of $3.5\times10^{-4}$ mol $L^{-1}$ of ECR on the sensitivity.

### 3.3.2.7 Effect of aspiration volumes of CTMAB on the sensitivity

The influence of the aspiration volumes of CTMAB on the sensitivity was tested over the range 50-150 μL. The results obtained are given in Table 3.27 and Figure 3.21. The sensitivity increased with an increase in the aspiration volume of CTMAB, but the sensitivity decreased dramatically for aspiration volume larger than 75 μL. A aspiration volume of 75 μL was chosen as the optimum due to the best sensitivity.

**Table 3.27** Effect of various aspiration volume of $2.5\times10^{-3}$ mol $L^{-1}$ of CTMAB on the sensitivity.

| Aspiration volume of CTMAB (μL) | Sensitivity (AU/mg $L^{-1}$) | | | | SD |
|---|---|---|---|---|---|
| | 1 | 2 | 3 | $\bar{x}^*$ | |
| 50 | 0.147 | 0.143 | 0.141 | 0.144 | 0.0030 |
| 75 | 0.199 | 0.202 | 0.201 | 0.201 | 0.0015 |
| 100 | 0.178 | 0.173 | 0.172 | 0.174 | 0.0032 |
| 125 | 0.168 | 0.165 | 0.168 | 0.167 | 0.0017 |
| 150 | 0.143 | 0.145 | 0.144 | 0.144 | 0.0010 |

*average of triplicate results

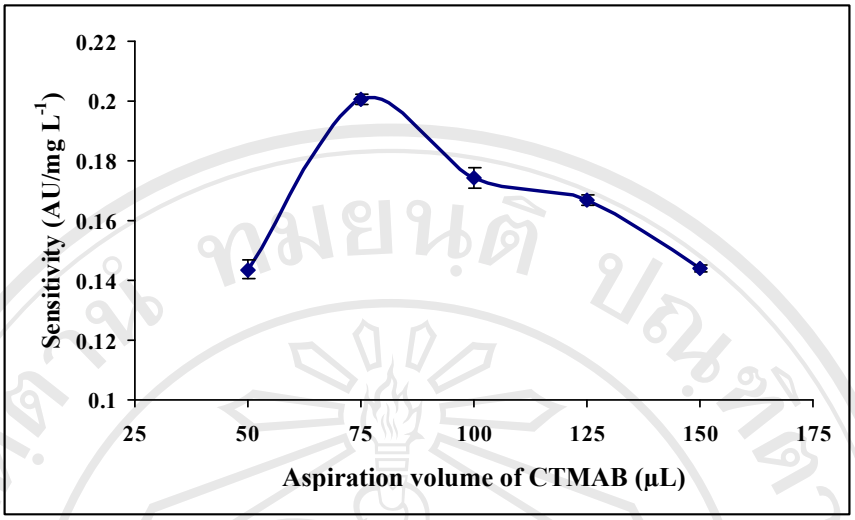


**Figure 3.21** Relationship between various aspiration volumes of $2.5\times10^{-3}$ mol $L^{-1}$ of CTMAB on the sensitivity of the calibration curve.

### 3.3.2.8 Effect of aspiration volumes of sample on the sensitivity

The sample aspiration volume ranging from 75 to 175 µL were evaluated. The results are shown in Table 3.28 and Figure 3.22. It was found that increasing the aspiration volumes of sample resulted in a subsequent increase in the sensitivity up to 125 µL after which the sensitivity began to decrease. Thus 125 µL of aspiration volumes of sample was used as the optimum concentration.

**Table 3.28** Effect of various aspiration volume of sample on the sensitivity.

| Aspiration volume of sample (µL) | Sensitivity (AU/mg $L^{-1}$) | | | | SD |
|---|---|---|---|---|---|
| | 1 | 2 | 3 | $\bar{x}$ * | |
| 75 | 0.105 | 0.119 | 0.117 | 0.114 | 0.0074 |
| 100 | 0.168 | 0.163 | 0.162 | 0.164 | 0.0032 |
| 125 | 0.237 | 0.226 | 0.239 | 0.234 | 0.0070 |
| 150 | 0.209 | 0.204 | 0.201 | 0.205 | 0.0040 |
| 175 | 0.147 | 0.143 | 0.145 | 0.145 | 0.0020 |

*average of triplicate results

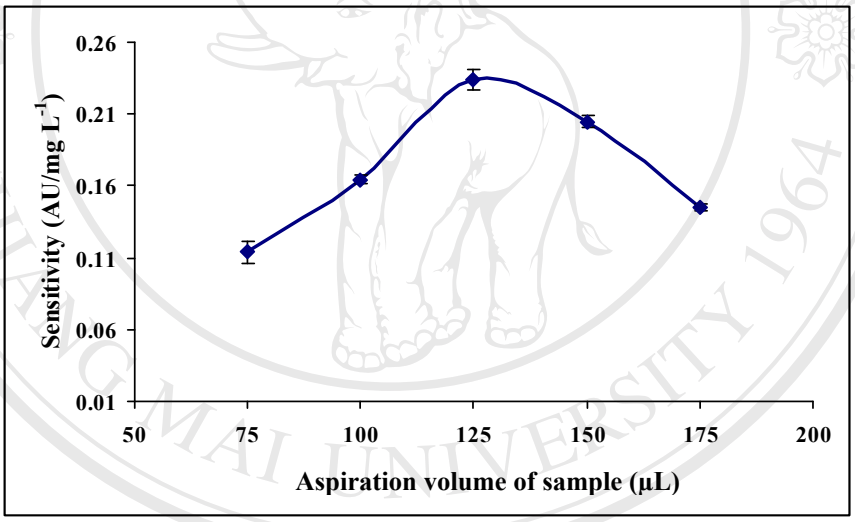


**Figure 3.22** Relationship between various aspiration volumes of standard solution of iron on the sensitivity of the calibration curve.

### 3.3.2.9 Effect of flow rate on the sensitivity

The flow rate in SIA is an extremely important parameter that has an influence on the amount of final products formed. The flow rate was evaluated between 50-175 μL $s^{-1}$ by changing the speed of the syringe pump. The results in Table 3.29 and Figure 3.23 revealed that there is slight increase in sensitivity from 50 to about 100 μL $s^{-1}$, and this shows that the reaction is fast and develop colour immediately. Beyond 100 μL $s^{-1}$ the sensitivity decreased. At high flow rate, i.e. above 100 μL $s^{-1}$ the flowing stream of reagent and sample solutions is so fast that the time for complex formation is limited and consequently insufficient complex is formed. The best sensitivity was found to be when the flow rate was from 50-175 μL $s^{-1}$ and 100 was chosen.

**Table 3.29** Effect of various flow rates on the sensitivity.

| Flow rate (μL $s^{-1}$) | Sensitivity (AU/mg $L^{-1}$) | | | | SD |
|---|---|---|---|---|---|
| | 1 | 2 | 3 | $\bar{x}$ * | |
| 50 | 0.210 | 0.211 | 0.208 | 0.210 | 0.0015 |
| 75 | 0.225 | 0.227 | 0.217 | 0.223 | 0.0053 |
| 100 | 0.228 | 0.232 | 0.229 | 0.230 | 0.0021 |
| 125 | 0.214 | 0.219 | 0.220 | 0.216 | 0.0032 |
| 150 | 0.168 | 0.166 | 0.164 | 0.166 | 0.0020 |
| 175 | 0.149 | 0.153 | 0.149 | 0.150 | 0.0023 |

*average of triplicate results

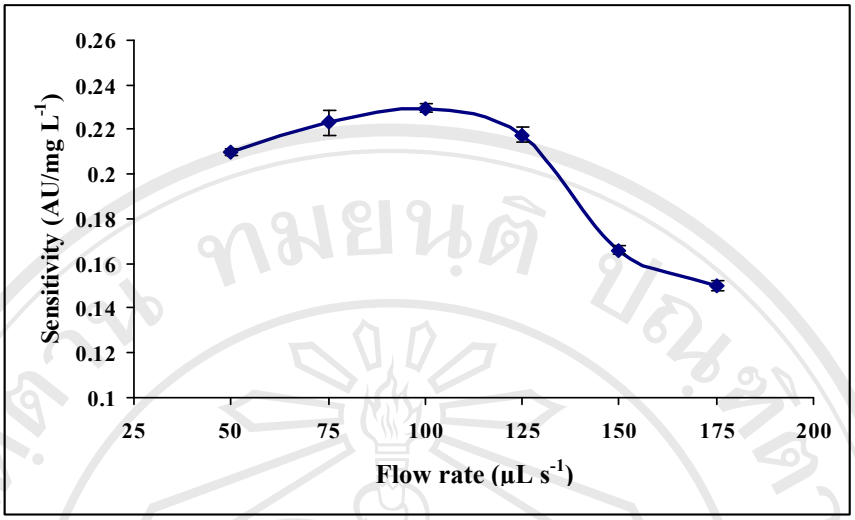


**Figure 3.23** Relationship between various flow rates on the sensitivity of the calibration curve.

### 3.3.2.10 Effect of holding coil length on the sensitivity

The holding coil is the region where different zones are stacked. The manner in which the zones are stacked has a strong bearing on the mixing and penetration of these zones as they are forwarded to the detector, consequently affecting the response of the system [71]. Thus the holding coil must be long enough to accommodate the stack of zones aspirated into it. The length of the holding coil was studied between 75 to 200 cm and the results are given in Table 3.30 and Figure 3.24, the length chosen is 150 cm as it displayed the highest sensitivity. A shorter holding coil leads to deformed peaks; a longer holding coil leads to increased dispersion on flow reversal.

**Table 3.30** Effect of various holding coil length on the sensitivity.

| Holding coil length (cm) | Sensitivity ( AU/mg $L^{-1}$) | | | | SD |
|---|---|---|---|---|---|
| | 1 | 2 | 3 | $\bar{x}$ * | |
| 75 | 0.229 | 231 | 233 | 0.231 | 0.0020 |
| 100 | 0.239 | 0.232 | 0.228 | 0.233 | 0.0056 |
| 125 | 0.273 | 0.262 | 0.268 | 0.268 | 0.0055 |
| 150 | 0.276 | 0.281 | 0.283 | 0.280 | 0.0036 |
| 175 | 0.225 | 0.227 | 0.230 | 0.227 | 0.0025 |
| 200 | 0.223 | 0.215 | 0.225 | 0.221 | 0.0053 |

*average of triplicate results

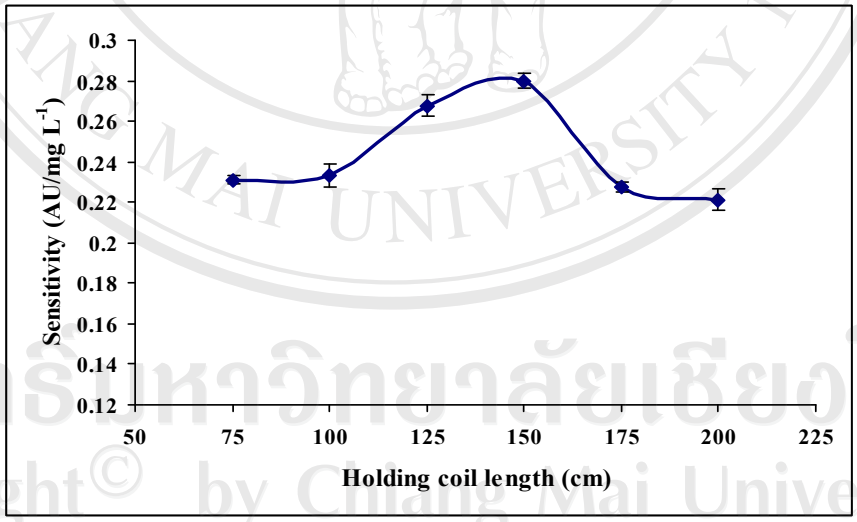


**Figure 3.24** Relationship between various holding coil lengths on the sensitivity of the calibration curve.

### 3.3.2.11 Effect of holding time on the sensitivity

After aspirating the solutions into the holding coil as described in the above mentioned procedure, they were kept for a period of time, before being dispensed to the detector. Table 3.31 and Figure 3.25 showed the effect of holding time to complete the complex of Fe-ECR-CTMAB. The holding time were varied from 5-25 s. The sensitivity was maximum when the holding time was 15 s. So 15 s was chosen as holding time.

**Table 3.31** Effect of various holding time on the sensitivity.

| Holding time (s) | Sensitivity (AU/mg $L^{-1}$) | | | | SD |
|---|---|---|---|---|---|
| | 1 | 2 | 3 | $\bar{x}$ * | |
| 5 | 0.201 | 0.198 | 0.202 | 0.200 | 0.0021 |
| 10 | 0.231 | 0.227 | 0.231 | 0.230 | 0.0023 |
| 15 | 0.241 | 0.239 | 0.239 | 0.240 | 0.0011 |
| 20 | 0.215 | 0.222 | 0.219 | 0.219 | 0.0035 |
| 25 | 0.189 | 0.183 | 0.186 | 0.186 | 0.0030 |

*average of triplicate results

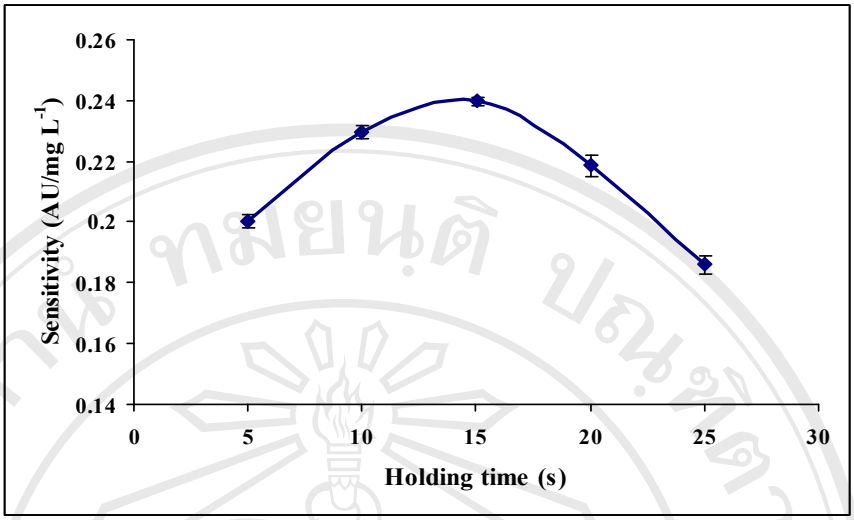


**Figure 3.25** Relationship between various holding times on the sensitivity of the calibration curve.

### 3.3.2.12 Effect of reaction coil length

The reaction coil between the selection value and detector is usually kept as short as possible to avoid excessive dilution of the formed product zone [70]. The effect of reaction coil length on determination of iron was studied by using Tygon tubings with a diameter of 1.07 mm i.d. with varying lengths of 0, 25, 50, 75 and 100 cm. The results are shown in Table 3.32 and Figure 3.26. The maximum sensitivity was obtained using a 50 cm of reaction coil length. After that the sensitivity decreased, because increasing of the length of reaction coil length will increased the distance to the detector yielding high dispersion. So, 50 cm coil length was required.

**Table 3.32** Effect of various reaction coil length on the sensitivity.

| Reaction coil length (cm) | Sensitivity (AU/mg $L^{-1}$) | | | | SD |
|---|---|---|---|---|---|
| | 1 | 2 | 3 | $\bar{x}^*$ | |
| 0 | 0.233 | 0.243 | 0.243 | 0.240 | 0.0058 |
| 25 | 0.251 | 0.253 | 0.263 | 0.256 | 0.0064 |
| 50 | 0.266 | 0.258 | 0.267 | 0.264 | 0.0049 |
| 75 | 0.237 | 0.243 | 0.245 | 0.242 | 0.0041 |
| 100 | 0.236 | 0.235 | 0.231 | 0.234 | 0.0026 |

*average of triplicate results

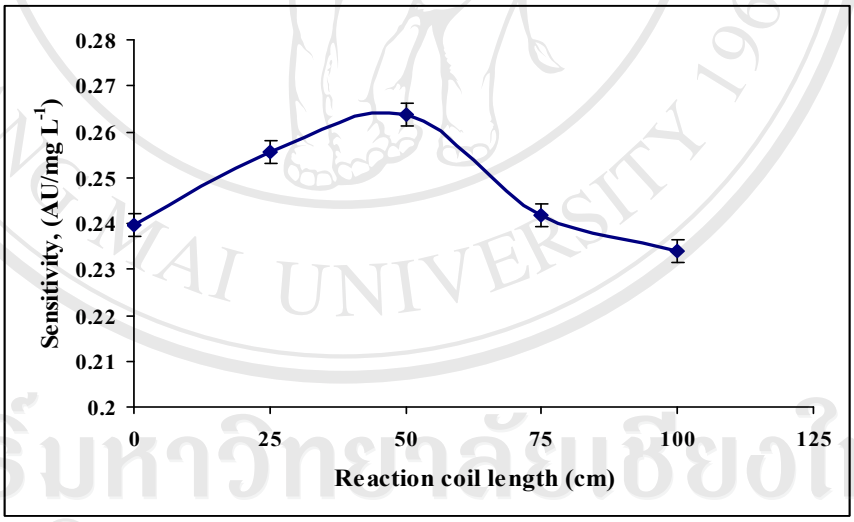


**Figure 3.26** Relationship between various reaction coil length on the sensitivity.

#### 3.3.2.13 Summary of the Studied Range and Optimum Conditions

Table 3.33 shows the ranges over which the variables involved in the SIA system were studied and their optimum values obtained by univariate optimization method.

**Table 3.33** Optimum conditions for iron determination.

| Variable | Studied range | Optimum value |
|---|---|---|
| pH | 4.0-6.0 | 5.5 |
| Concentration of pH (mol $L^{-1}$) | 0.01-0.2 | 0.1 |
| Concentration of ECR (x $10^{-4}$ mol $L^{-1}$) | 2.5-4.5 | 3.5 |
| Concentration of CTMAB (x $10^{-3}$ mol $L^{-1}$) | 1.0-3.0 | 2.5 |
| Aspiration volume of buffer (μL) | 25-125 | 50 |
| Aspiration volume of ECR (μL) | 100-225 | 175 |
| Aspiration volume of CTMAB (μL) | 50-150 | 75 |
| Aspiration volume of sample (μL) | 75-175 | 125 |
| Flow rate (μL $s^{-1}$) | 50-175 | 100 |
| Holding coil length (cm) | 75-200 | 150 |
| Holding time (s) | 5-25 | 15 |
| Reaction coil length (cm) | 0-100 | 50 |

### 3.3.3 Analytical Characteristics of the method

#### 3.3.3.1 Linear range

Using the SIA manifold (Figure 2.2) and under the optimum conditions in Table 3.33, the linear range of calibration graph was obtained from the results for several iron standards in the concentration ranging from 0-2.0 mg $L^{-1}$. All measurements were made in pentaplicate injections. The results obtained are shown in Table 3.34 and Figure 3.27.

**Table 3.34** Linearity of iron determination.

| Iron (mg $L^{-1}$) | Peak height (AU) | | | | | | ΔP.H.* (AU) |
|---|---|---|---|---|---|---|---|
| | 1 | 2 | 3 | 4 | 5 | $\bar{x}$ | |
| 0.00 | 0.014 | 0.015 | 0.016 | 0.014 | 0.014 | 0.015 | 0.000 |
| 0.02 | 0.018 | 0.019 | 0.019 | 0.018 | 0.018 | 0.018 | 0.004 |
| 0.04 | 0.022 | 0.022 | 0.021 | 0.021 | 0.022 | 0.022 | 0.007 |
| 0.06 | 0.025 | 0.026 | 0.025 | 0.026 | 0.026 | 0.026 | 0.011 |
| 0.08 | 0.029 | 0.029 | 0.031 | 0.031 | 0.031 | 0.030 | 0.016 |
| 0.10 | 0.036 | 0.035 | 0.034 | 0.036 | 0.034 | 0.035 | 0.020 |
| 0.15 | 0.047 | 0.047 | 0.049 | 0.047 | 0.048 | 0.048 | 0.033 |
| 0.20 | 0.059 | 0.059 | 0.058 | 0.06 | 0.059 | 0.059 | 0.044 |
| 0.25 | 0.072 | 0.071 | 0.072 | 0.071 | 0.073 | 0.072 | 0.057 |
| 0.30 | 0.081 | 0.081 | 0.083 | 0.081 | 0.082 | 0.082 | 0.067 |
| 0.35 | 0.093 | 0.092 | 0.095 | 0.092 | 0.095 | 0.093 | 0.079 |
| 0.40 | 0.106 | 0.105 | 0.104 | 0.104 | 0.105 | 0.105 | 0.090 |
| 0.45 | 0.116 | 0.118 | 0.119 | 0.117 | 0.118 | 0.118 | 0.103 |

*average of pentaplicate results

**Table 3.34** (Continued).

| Iron (mg $L^{-1}$) | Peak height (AU) | | | | | | ΔP.H.* (AU) |
|---|---|---|---|---|---|---|---|
| | 1 | 2 | 3 | 4 | 5 | $\bar{x}$ | |
| 0.50 | 0.123 | 0.122 | 0.121 | 0.123 | 0.121 | 0.122 | 0.107 |
| 0.55 | 0.129 | 0.130 | 0.128 | 0.127 | 0.129 | 0.129 | 0.114 |
| 0.60 | 0.134 | 0.134 | 0.136 | 0.136 | 0.136 | 0.135 | 0.121 |
| 0.65 | 0.141 | 0.143 | 0.143 | 0.144 | 0.142 | 0.143 | 0.128 |
| 0.70 | 0.151 | 0.150 | 0.150 | 0.149 | 0.150 | 0.150 | 0.135 |
| 0.75 | 0.155 | 0.156 | 0.157 | 0.155 | 0.155 | 0.156 | 0.141 |
| 0.80 | 0.161 | 0.164 | 0.162 | 0.162 | 0.163 | 0.162 | 0.148 |
| 0.85 | 0.167 | 0.167 | 0.168 | 0.167 | 0.168 | 0.167 | 0.153 |
| 0.90 | 0.174 | 0.171 | 0.173 | 0.171 | 0.173 | 0.172 | 0.159 |
| 0.95 | 0.177 | 0.178 | 0.177 | 0.177 | 0.178 | 0.177 | 0.163 |
| 1.00 | 0.182 | 0.181 | 0.181 | 0.182 | 0.183 | 0.182 | 0.167 |
| 1.25 | 0.207 | 0.208 | 0.206 | 0.208 | 0.206 | 0.207 | 0.192 |
| 1.50 | 0.231 | 0.232 | 0.229 | 0.231 | 0.231 | 0.231 | 0.216 |
| 1.75 | 0.253 | 0.254 | 0.253 | 0.252 | 0.253 | 0.253 | 0.238 |
| 2.00 | 0.265 | 0.267 | 0.268 | 0.265 | 0.265 | 0.266 | 0.251 |

*average of pentaplicate results

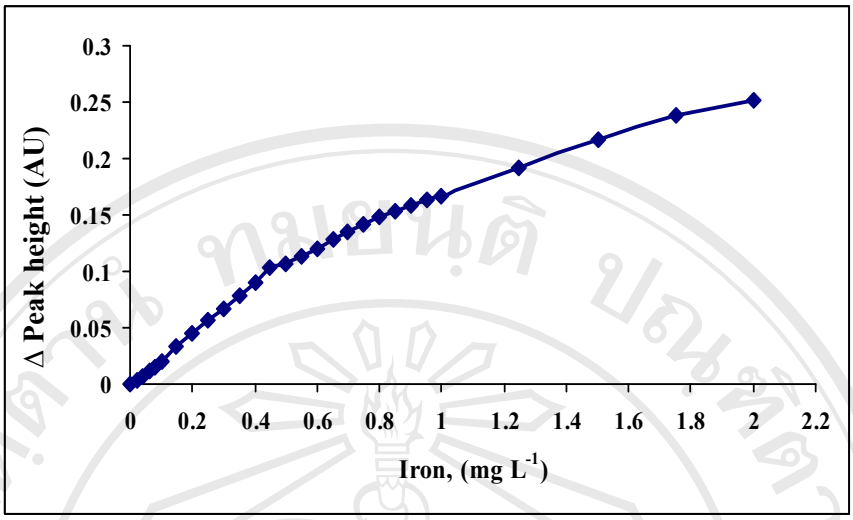


**Figure 3.27** Relationship between Δpeak height and concentration of iron.

### 3.3.3.2 Calibration curve

The linearity of the sequential injection method for the determination of iron (III) was studied under optimum conditions as shown in Table 3.33, the calibration graph were linear for 0.02-0.45 mg $L^{-1}$ iron ($r^2$ = 0.9995) and 0.45-1.0 mg $L^{-1}$ iron ($r^2$=0.9948), respectively. The results obtained are shown in Table 3.35 and Figure 3.28-3.29. Over these two concentration ranges, linear regression analysis of iron as Fe: ECR: CTMAB peak height (y) versus iron concentration (x) yields the following equations:

$$Y = 0.2325x + 0.0022 \ (r^2 = 0.9995) \ \text{(Fe (III) 0.02-0.45 mg } L^{-1})$$

$$Y = 0.1210x + 0.0632 \ (r^2 = 0.9948) \ \text{(Fe (III) 0.45-1.0 mg } L^{-1})$$

Where: y = Δpeak height in Absorbance (AU)

x = concentration of iron in mg $L^{-1}$

**Table 3.35** ΔPeak height for calibration curve.

| Iron (mg $L^{-1}$) | Peak height (AU) | | | | | | ΔP.H.* (AU) |
|---|---|---|---|---|---|---|---|
| | 1 | 2 | 3 | 4 | 5 | $\bar{x}$ | |
| 0.00 | 0.014 | 0.015 | 0.016 | 0.014 | 0.014 | 0.015 | 0.000 |
| 0.02 | 0.018 | 0.019 | 0.019 | 0.018 | 0.018 | 0.018 | 0.004 |
| 0.04 | 0.022 | 0.022 | 0.021 | 0.021 | 0.022 | 0.022 | 0.007 |
| 0.08 | 0.029 | 0.029 | 0.031 | 0.031 | 0.031 | 0.030 | 0.016 |
| 0.10 | 0.036 | 0.035 | 0.034 | 0.036 | 0.034 | 0.035 | 0.020 |
| 0.15 | 0.047 | 0.047 | 0.049 | 0.047 | 0.048 | 0.048 | 0.033 |
| 0.20 | 0.059 | 0.059 | 0.058 | 0.06 | 0.059 | 0.059 | 0.044 |
| 0.25 | 0.072 | 0.071 | 0.072 | 0.071 | 0.073 | 0.072 | 0.057 |
| 0.30 | 0.081 | 0.081 | 0.083 | 0.081 | 0.082 | 0.082 | 0.067 |
| 0.35 | 0.093 | 0.092 | 0.095 | 0.092 | 0.095 | 0.093 | 0.079 |
| 0.40 | 0.106 | 0.105 | 0.104 | 0.104 | 0.105 | 0.105 | 0.090 |
| 0.45 | 0.116 | 0.118 | 0.119 | 0.117 | 0.118 | 0.118 | 0.103 |
| 0.50 | 0.123 | 0.122 | 0.121 | 0.123 | 0.121 | 0.122 | 0.107 |
| 0.60 | 0.134 | 0.134 | 0.136 | 0.136 | 0.136 | 0.135 | 0.121 |
| 0.70 | 0.151 | 0.150 | 0.150 | 0.149 | 0.150 | 0.150 | 0.135 |
| 0.80 | 0.161 | 0.164 | 0.162 | 0.162 | 0.163 | 0.162 | 0.148 |
| 0.90 | 0.174 | 0.171 | 0.173 | 0.171 | 0.173 | 0.172 | 0.159 |
| 1.00 | 0.182 | 0.181 | 0.181 | 0.182 | 0.183 | 0.182 | 0.167 |

* average of pentaplicate results

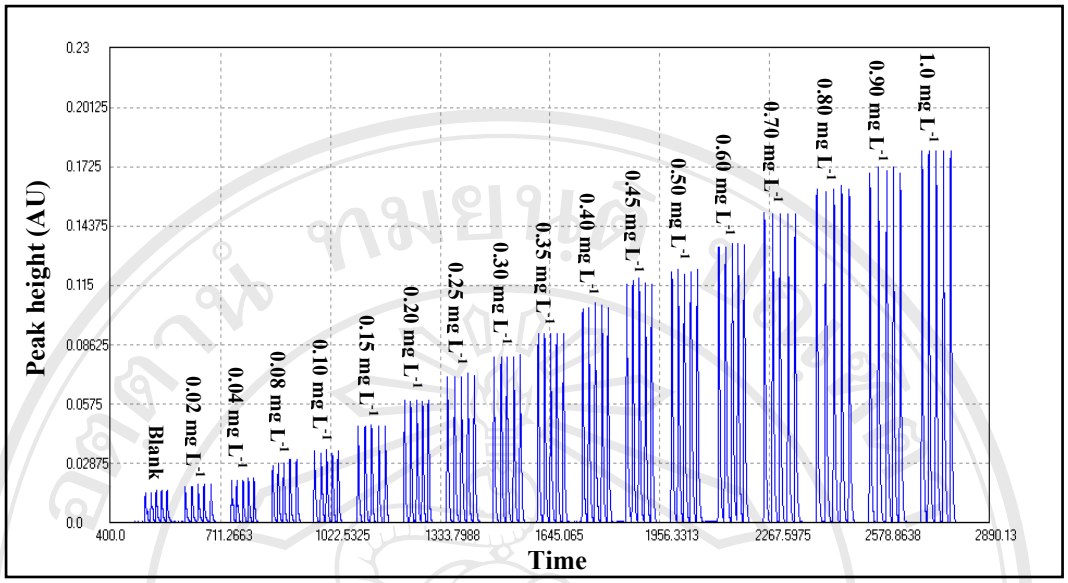


**Figure 3.28** Calibration signal of SIA spectrophotometric determination of iron 0.02-0.45 and 0.45-1.0 mg $L^{-1}$.

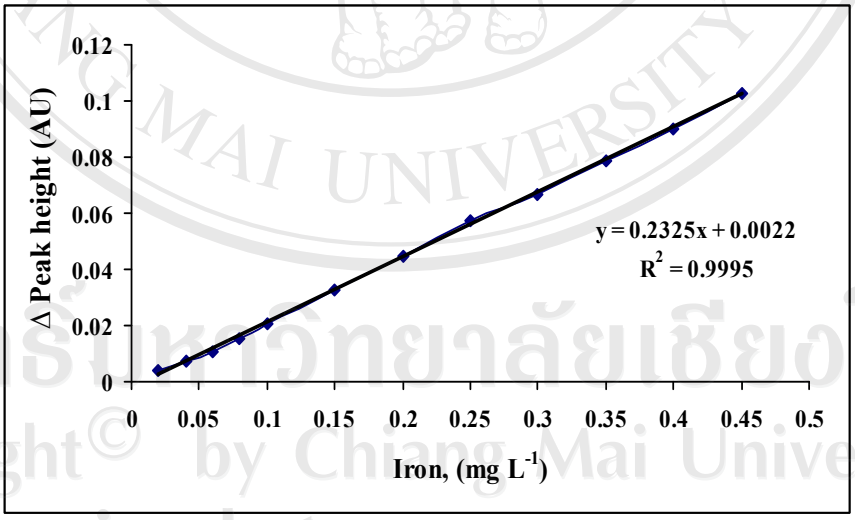


(a)

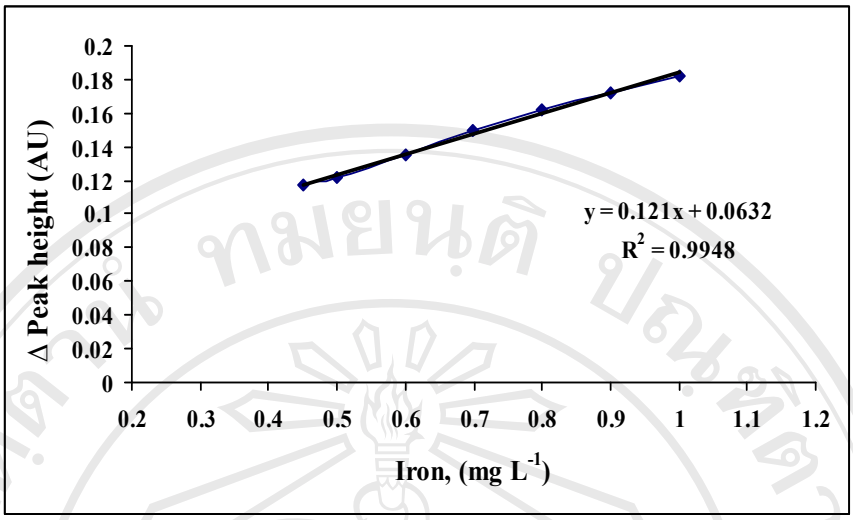


(b)

**Figure 3.29** The calibration curve of SIA spectrophotometric determination of iron: (a) iron 0.02-0.45 mg $L^{-1}$; (b) iron 0.45–1.0 mg $L^{-1}$.

### 3.3.3.3 Precision of the sequential injection system

The precision of the proposed SIA system was determination by 11 replicated analysis of a number of standard iron (III) solutions as indicated in Table 3.36. The percentage relative standard deviation (RSD) for 0.04, 0.1, 0.5 and 1.0 mg $L^{-1}$ of iron was found to be 2.17, 2.25, 0.85 and 0.38 %, respectively.

**Table 3.36** Precision verification using various concentrations of iron standard.

| Experimental number | Peak height (AU) obtained from the standard Fe(III) (mg $L^{-1}$) | | | |
|---|---|---|---|---|
| | **0.04** | **0.10** | **0.5** | **1.0** |
| 1 | 0.023 | 0.030 | 0.116 | 0.181 |
| 2 | 0.023 | 0.032 | 0.116 | 0.181 |
| 3 | 0.023 | 0.030 | 0.117 | 0.181 |
| 4 | 0.023 | 0.031 | 0.116 | 0.182 |
| 5 | 0.022 | 0.030 | 0.117 | 0.181 |
| 6 | 0.023 | 0.031 | 0.116 | 0.182 |
| 7 | 0.022 | 0.031 | 0.117 | 0.181 |
| 8 | 0.023 | 0.030 | 0.117 | 0.181 |
| 9 | 0.023 | 0.032 | 0.117 | 0.183 |
| 10 | 0.022 | 0.030 | 0.120 | 0.181 |
| 11 | 0.023 | 0.031 | 0.119 | 0.182 |
| $\overline{X}$ | 0.023 | 0.031 | 0.117 | 0.181 |
| S.D. | 0.0005 | 0.0007 | 0.0011 | 0.0007 |
| % R.S.D. | 2.17 | 2.25 | 0.85 | 0.38 |

### 3.3.3.4 Detection limit

The detection limit gives an indication of the lowest iron (III) concentration that cab be distinguished from the blank signal or background signal [67]. The detection limit was calculated using the relation $[3(\sigma + k) - c]/m$, where σ (0.0009) is the standard deviation of the background signal, $k$ (0.0000) is the average signal value of the baseline and $c$ (0.0022) and $m$ (0.2052) are the intercept and the slope of the calibration curve, respectively. The calculated detection limit was found to be 0.012 mg $L^{-1}$ as shown in Table 3.37.

**Table 3.37** The blank signal resulting from 12 injections.

| Experimental number | Peak height (AU) * |
|---|---|
| 1 | 0.014 |
| 2 | 0.014 |
| 3 | 0.013 |
| 4 | 0.013 |
| 5 | 0.013 |
| 6 | 0.014 |
| 7 | 0.014 |
| 8 | 0.015 |
| 9 | 0.014 |
| 10 | 0.015 |
| 11 | 0.015 |
| 12 | 0.015 |
| $\overline{X}$ | 0.014 |
| S.D. | 0.0009 |
| LOD (mg $L^{-1}$) | 0.012 |

*average of triplicate results

### 3.3.3.5 Interference Studies

The influences of various cations ($Al^{3+}$, $Ca^{2+}$, $Cu^{2+}$, $Co^{2+}$, $Cr^{3+}$, $Fe^{2+}$, $Mg^{2+}$, $Mn^{2+}$, $Zn^{2+}$, $Na^{+}$, $Ni^{2+}$) and anions ($Br^{-}$, $Cl^{-}$, $HCO_3^{-}$, $I^{-}$, $NO_2^{-}$, $NO_3^{-}$, $PO_4^{3-}$, $SO_4^{2-}$) commonly associated with analytes were investigated. The effects of some possible interfering ions on the determination of 0.2 mg $L^{-1}$ iron were studied for the maximum w/w ratio of interfering ions to iron up to 1000:1. The tolerance value (defined as the foreign-ion concentration causing an error smaller than ±10% for determining the analyte of interest) for the ions studied are listed in Table 3.38.

**Table 3.38** Interference studies for 0.2 mg $L^{-1}$ standard iron by SIA method.

| Ions | Chemical form added | Concentration added (mg $L^{-1}$) | Peak height (AU)* | % Relative Error |
|---|---|---|---|---|
| none | - | - | 0.045 | - |
| $Al^{3+}$ | $Al(NO_3)_2$ | 0.10 | 0.050 | +4.87 |
| | | 0.15 | 0.054 | +9.73 |
| | | 0.20 | 0.058 | +19.03 |
| | | 0.25 | 0.060 | +28.76 |
| | | 0.30 | 0.063 | +33.18 |
| $Ca^{2+}$ | $Ca(NO_3)_2$ | 300 | 0.045 | -1.33 |
| | | 500 | 0.044 | -2.21 |
| | | 800 | 0.043 | -3.98 |
| | | 900 | 0.042 | -6.19 |
| | | 1000 | 0.041 | -9.73 |
| $Cu^{2+}$ | $Cu(NO_3)_2$ | 10 | 0.048 | +5.75 |
| | | 15 | 0.050 | +8.85 |
| | | 20 | 0.051 | +12.83 |
| | | 25 | 0.055 | +21.68 |
| | | 30 | 0.056 | +24.34 |

**Table 3.38** (Continued).

| Ions | Chemical form added | Concentration added (mg $L^{-1}$) | Peak height (AU)* | % Relative Error |
|---|---|---|---|---|
| none | - | - | 0.045 | - |
| $Co^{2+}$ | $Co(NO_3)_2$ | 300 | 0.043 | -4.42 |
| | | 500 | 0.043 | -4.42 |
| | | 600 | 0.042 | -6.64 |
| | | 700 | 0.041 | -9.73 |
| | | 800 | 0.039 | -13.27 |
| $Cr^{3+}$ | $Cr(NO_3)_2$ | 5 | 0.046 | +2.21 |
| | | 10 | 0.048 | +7.08 |
| | | 15 | 0.049 | +9.29 |
| | | 30 | 0.050 | +11.06 |
| | | 40 | 0.053 | +16.81 |
| $Mg^{2+}$ | $Mg(NO_3)_2$ | 300 | 0.043 | -5.75 |
| | | 500 | 0.043 | -5.75 |
| | | 700 | 0.042 | -6.19 |
| | | 900 | 0.041 | -9.73 |
| | | 1000 | 0.040 | -11.50 |
| $Mn^{2+}$ | $Mn(NO_3)_2$ | 100 | 0.046 | +1.77 |
| | | 200 | 0.047 | +3.98 |
| | | 300 | 0.049 | +7.96 |
| | | 400 | 0.050 | +9.73 |
| | | 500 | 0.051 | +12.39 |
| $Na^{+}$ | $NaNO_3$ | 100 | 0.044 | -1.77 |
| | | 300 | 0.043 | -5.75 |
| | | 500 | 0.041 | -8.85 |
| | | 600 | 0.038 | -15.93 |
| | | 700 | 0.036 | -19.47 |

**Table 3.38** (Continued).

| Ions | Chemical form added | Concentration added (mg $L^{-1}$) | Peak height (AU)* | % Relative Error |
|---|---|---|---|---|
| none | - | - | 0.045 | - |
| $Ni^{2+}$ | $Ni(NO_3)_2$ | 100 | 0.044 | -3.09 |
| | | 200 | 0.042 | -7.52 |
| | | 300 | 0.041 | -9.73 |
| | | 500 | 0.041 | -9.73 |
| | | 600 | 0.039 | -14.16 |
| $Zn^{2+}$ | $Zn(NO_3)_2$ | 100 | 0.043 | -5.75 |
| | | 200 | 0.043 | -5.75 |
| | | 300 | 0.041 | -9.73 |
| | | 400 | 0.039 | -13.72 |
| | | 500 | 0.036 | -19.91 |
| $Br^-$ | NaBr | 100 | 0.045 | 0 |
| | | 300 | 0.045 | 0 |
| | | 500 | 0.045 | 0 |
| | | 800 | 0.043 | -5.75 |
| | | 1000 | 0.040 | -11.50 |
| $Cl^-$ | NaCl | 100 | 0.045 | 0 |
| | | 300 | 0.045 | 0 |
| | | 500 | 0.045 | 0 |
| | | 800 | 0.045 | 0 |
| | | 1000 | 0.045 | 0 |
| $HCO_3^-$ | $NaHCO_3$ | 50 | 0.044 | -3.10 |
| | | 100 | 0.043 | -5.31 |
| | | 150 | 0.041 | -9.29 |
| | | 200 | 0.039 | -13.72 |
| | | 300 | 0.020 | -56.19 |

**Table 3.38** (Continued).

| Ions | Chemical form added | Concentration added (mg $L^{-1}$) | Peak height (AU)* | % Relative Error |
|---|---|---|---|---|
| none | - | - | 0.045 | - |
| $I^-$ | NaI | 1 | 0.043 | -5.31 |
| | | 5 | 0.042 | -6.64 |
| | | 10 | 0.041 | -10.18 |
| | | 15 | 0.039 | -12.83 |
| | | 20 | 0.039 | -12.83 |
| $NO_2^-$ | $NaNO_2$ | 5 | 0.047 | +3.54 |
| | | 10 | 0.049 | +7.52 |
| | | 15 | 0.050 | +10.62 |
| | | 20 | 0.052 | +15.93 |
| | | 30 | 0.054 | +19.47 |
| $NO_3^-$ | $NaNO_3$ | 100 | 0.045 | 0 |
| | | 300 | 0.045 | 0 |
| | | 500 | 0.044 | -1.77 |
| | | 800 | 0.043 | -3.98 |
| | | 1000 | 0.041 | -8.41 |
| $PO_4^{3-}$ | $Na_3PO_4 \cdot 12H_2O$ | 200 | 0.044 | -1.32 |
| | | 300 | 0.043 | -4.42 |
| | | 330 | 0.042 | -7.08 |
| | | 350 | 0.041 | -10.18 |
| | | 370 | 0.039 | -13.27 |
| $SO_4^{2-}$ | $Na_2SO_4$ | 100 | 0.046 | +1.77 |
| | | 300 | 0.047 | +3.03 |
| | | 500 | 0.049 | +7.91 |
| | | 800 | 0.045 | +9.29 |
| | | 1000 | 0.045 | +9. 29 |

*average of triplicate results

The interference effects of some possible foreign ions in the SIA system for iron were summarized in Table 3.39. It was found $Al^{3+}$ interfered determination iron in bottled-drinking water, which referred standard quality of bottled-drinking water defined by pollution control department, ministry of natural resources and environment (WHO 2006) [72]. (Appendix A). So, aluminum in the water samples was eliminated by the addition of sodium fluoride as the masking agent [69].

**Table 3.39** Summary of interference effects of some ions on the response obtained from iron 0.2 mg $L^{-1}$ by SIA method.

| **Interference ions** | **Tolerable concentration ratio* (mg $L^{-1}$) of ion/Fe (III)** |
|---|---|
| $Ca^{2+}$, $Br^-$, $Cl^-$, $SO_4^{2-}$, $NO_3^-$ | ≥1000 |
| $Mg^{2+}$ | 900 |
| $Co^{2+}$ | 700 |
| $Na^+$, $Ni^{2+}$, | 500 |
| $Mn^{2+}$ | 400 |
| $PO_4^{3-}$ | 350 |
| $Zn^{2+}$ | 300 |
| $HCO_3^-$ | 150 |
| $Cu^{2+}$, $Cr^{3+}$, $NO_2^-$ | 15 |
| $I^-$ | 10 |
| $Al^{3+}$ | <1 |

*The concentration of an ion is considered to be interfering when causing a relative error of more than ±10% with respect to the signal of Fe (III) alone.

### 3.3.3.6 Effect of masking agents and interference

The effect of masking agent and interference was studied by the proposed SIA under the optimum conditions. In order to reduce interference effects of $Al^{3+}$. A concentration of NaF as making agent for Fe (III) determination was investigated. The results are shown in Table 3.40. The result indicated that at 0.0006 mol $L^{-1}$ of sodium fluoride is the optimum concentration which does not affect the sensitivity. The interference from aluminum up to 1.5 mg $L^{-1}$ was completely removed by adding 0.0006 mol $L^{-1}$ sodium fluoride.

**Table 3.40** Effect of masking agent for mask $Al^{3+}$ the response obtained from Fe (III) 0.2 mg $L^{-1}$ by SIA method.

| Interference | Concentration of masking agent | Iron : Interference | Peak height (Abs.) | % Relative Error |
|---|---|---|---|---|
| $Al^{3+}$ | 0.0004 mol $L^{-1}$ $F^-$ | 1:0 | 0.045 | - |
| | | 1:1 | 0.048 | +5.31 |
| | | 1:5 | 0.049 | +7.08 |
| | | 1:7.5 | 0.050 | +10.17 |
| | | 1:10 | 0.052 | +16.81 |
| | 0.0006 mol $L^{-1}$ $F^-$ | 1:0 | 0.045 | - |
| | | 1:1 | 0.047 | +3.10 |
| | | 1:5 | 0.048 | +6.19 |
| | | 1:7.5 | 0.049 | +8.85 |
| | | 1:10 | 0.051 | +12.39 |
| | 0.0008 mol $L^{-1}$ $F^-$ | 1:0 | 0.045 | - |
| | | 1:1 | 0.047 | +3.10 |
| | | 1:5 | 0.049 | +7.52 |
| | | 1:7.5 | 0.050 | +10.18 |
| | | 1:10 | 0.051 | +12.80 |

*average of triplicate results

### 3.3.3.7 Determination of iron in drinking waters

The proposed SIA spectrophotometric method was applied to the simultaneous determination of iron in drinking water samples which were commercial drinking waters available in the market around Chiang Mai Municipality. The peak heights from each sample were compared with standard calibration curve. The results were given in Table 3.41.

**Table 3.41** Determination of iron in drinking water sample by SIA method.

| Water samples brand | Peak heights | | | | SD | Iron concentration* (mg $L^{-1}$) | % recovery* |
|---|---|---|---|---|---|---|---|
| | 1 | 2 | 3 | $\overline{X}$ | | | |
| Amtech | 0.005 | 0.007 | 0.007 | 0.006 | 0.001 | 0.006 ± 0.001 | 104.85 |
| Big Bell | 0.017 | 0.016 | 0.015 | 0.016 | 0.001 | 0.016 ± 0.001 | 104.04 |
| Double Elephants | 0.012 | 0.011 | 0.014 | 0.012 | 0.002 | 0.012 ± 0.002 | 103.50 |
| F&B | ND** | ND** | ND** | - | - | ND** | - |
| Free Bird | ND** | ND** | ND** | - | - | ND** | - |
| Mont Blanc | 0.008 | 0.009 | 0.009 | 0.009 | 0.001 | 0.009 ± 0.001 | 101.05 |
| Nam Petch | 0.006 | 0.005 | 0.006 | 0.006 | 0.001 | 0.006 ± 0.001 | 102.67 |
| Nasibee | 0.017 | 0.016 | 0.019 | 0.017 | 0.002 | 0.017 ± 0.002 | 99.70 |
| Pola | ND** | ND** | ND** | - | - | ND** | - |
| Polestar | 0.006 | 0.007 | 0.006 | 0.006 | 0.001 | 0.006 ± 0.001 | 98.75 |
| Rrintip | ND** | ND** | ND** | - | - | ND** | - |
| Wang Nam Kang | 0.011 | 0.008 | 0.009 | 0.009 | 0.002 | 0.009 ± 0.002 | 99.93 |

*average of triplicate results

**not detected

The iron contents in drinking water samples were in the range 0.006-0.017 mg $L^{-1}$ and <0.0005-0.018 mg $L^{-1}$ using the proposed method and ICP-MS (Agilent 7500 C) respectively. The results obtained by the proposed SIA spectrophotometric method compared with those obtained by ICP-MS using the student *t*-test (Table 3.42) and Appendix B in Table B.1). It was evident that the *t*-value for Fe (III) contents in drinking water samples determined by comparison the results obtained by SIA spectrophotometric with those obtained by ICP-MS were -1.500, -1.732, -0.730, -3.266, -1.001, -0.756, -1.633 and -0.756, for samples Amtech, Big Bell, Double Elephants, Mont Blanc, Nam Petch Nasibee, Polestar and Wang Nam Kang, respectively. It was seen that experimental *t*-value for Fe(III) assay, which was smaller than the theoretical *t*-value at a confidence interval of 95% (4.30) indicating that results obtained by both methods were in excellent agreement.

**Table 3.42** Comparative determination of iron in drinking water sample by proposed SIA method and ICP-MS.

| **Drinking water sample** | **Concentrations (mg $L^{-1}$)** | | $t_{calculated}$ |
|---|---|---|---|
| | **SIA*** | **ICP-MS*** | |
| Amtech | 0.006 | 0.007 | -1.500 |
| Big Bell | 0.016 | 0.017 | -1.732 |
| Double Elephants | 0.012 | 0.013 | -0.730 |
| F&B | ND** | <0.0005 | - |
| Free Bird | ND** | <0.0005 | - |
| Mont Blanc | 0.009 | 0.010 | -3.266 |
| Nam Petch | 0.006 | 0.006 | -1.001 |
| Nasibee | 0.017 | 0.018 | -0.756 |
| Pola | ND** | <0.0005 | - |
| Polestar | 0.006 | 0.007 | -1.633 |
| Rrintip | ND** | <0.0005 | - |
| Wang Nam Kang | 0.009 | 0.010 | -0.756 |

*average of triplicate results
**not detected